

Medieval Warm Period

Related terms:

[Holocene](#), [Little Ice Age](#), [Tree Ring](#), [Boreholes](#), [Northern Hemisphere](#)

[View all Topics](#)

Learn more about Medieval Warm Period

Geologic Evidence of Recurring Climate Cycles and Their Implications for the Cause of Global Climate Changes—The Past is the Key to the Future

Don J. Easterbrook, in [Evidence-Based Climate Science](#), 2011

5.1.1.6 The Medieval Warm Period (900 A.D. to 1300 A.D.)

The [Medieval Warm Period](#) (MWP) was a time of warm climate from about 900 A.D. to 1300 A.D. when global temperatures were apparently somewhat warmer than at present. Its effects were evident in Europe where [grain crops](#) flourished, alpine tree lines rose, many new cities arose, and the population more than doubled. The Vikings took advantage of the climatic [amelioration](#) to colonize Greenland, and wine grapes were grown as far north as England where growing grapes is now not feasible and about 500 km north of present [vineyards](#) in France and Germany. Grapes are presently grown in Germany up to elevations of about 560 m, but from about 1100 A.D. to 1300 A.D., vineyards extended up to 780 m, implying temperatures warmer by about 1.0–1.4 °C (Oliver, 1973). Wheat and oats were grown around Trondheim, Norway, suggesting climates about 1 °C warmer than present (Fagan, 2000).

Elsewhere in the world, prolonged [droughts](#) affected the southwestern United States and Alaska warmed. Sediments in central Japan record warmer temperatures. [Sea](#)

surface temperatures in the Sargasso Sea were approximately 1 °C warmer than today, and the climate in equatorial east Africa was drier from 1000 A.D. to 1270 A.D. An ice core from the eastern Antarctic Peninsula shows warmer temperatures during this period.

Oxygen isotope studies in Greenland, Ireland, Germany, Switzerland, Tibet, China, New Zealand, and elsewhere, plus tree-ring data from many sites around the world all confirm the presence of a global Medieval Warm Period. Soon and Baliunas (2003) found that 92% of 112 studies showed physical evidence of the MWP, only two showed no evidence, and 21 of 22 studies in the Southern Hemisphere showed evidence of Medieval warming. Evidence of the MWP at specific sites is summarized in Fagan (2007) and Singer and Avery (2007). Evidence that the Medieval Warm Period was a global event is so widespread that one wonders why Mann et al. (1998) ignored it.

The Hockey Stick Trick

Over a period of many decades, several thousand papers were published establishing the Medieval Warm Period (MWP) from about 900 A.D. to 1300 A.D. and the Little Ice Age (LIA) from about 1300 A.D. to 1915 A.D. as global climate changes. Thus, it came as quite a surprise when Mann et al. (1998) (Fig. 28) concluded that neither the MWP nor the Little Ice Age actually happened on the basis of a tree-ring study and that became the official position of the 2001 Intergovernmental Panel on Climate Change (IPCC). The IPCC 3rd report (Climate Change 2001) then totally ignored the several thousand publications detailing the global climate changes during the MWP and the LIA and used the Mann et al. tree-ring study as the basis for the now famous assertion that “*Our civilization has never experienced any environmental shift remotely similar to this. Today's climate pattern has existed throughout the entire history of human civilization.*” (Gore, 2007). This claim was used as the main evidence that increasing atmospheric CO₂ was causing global warming so, as revealed in the ‘Climategate’ scandal, advocates of the CO₂ theory were very concerned about the strength of data that showed the Medieval Warm Period (MWP) was warmer than the 20th century and that global warming had occurred naturally, long before atmospheric CO₂ began to increase. The contrived elimination of the MWP and Little Ice Age by Mann et al. became known as “the hockey stick” of climate change where the handle of the hockey stick was supposed to represent constant climate until increasing CO₂ levels caused global warming, the sharp bend in the lower hockey stick.

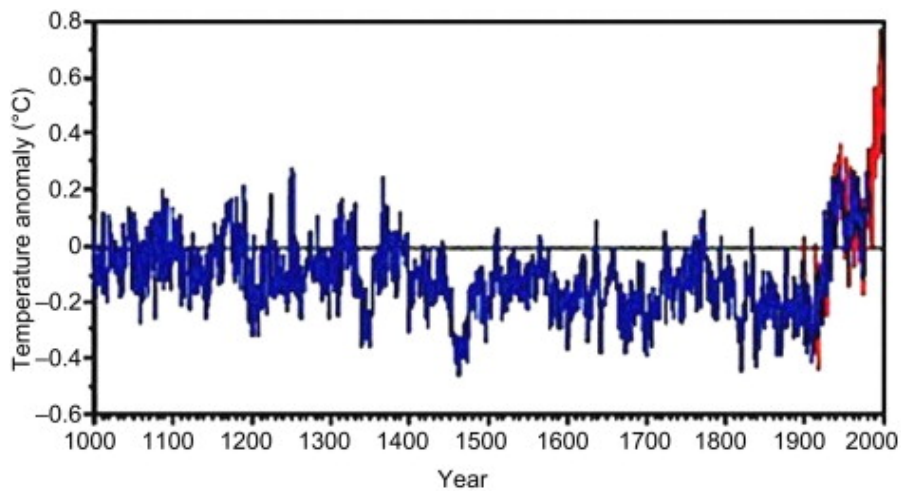


FIGURE 28. Mann et al. (1998) “hockey stick” graph of temperature change over the past 1,000 years based on tree rings.

The Mann et al. “hockey stick” temperature curve was at so at odds with thousands of published papers, including the Greenland GRIP ice core isotope data, [sea surface temperatures](#) in the Sargasso Sea sediments (Fig. 29) (Keigwin, 1996), paleo-temperature data other than tree rings (Fig. 30) (Loehle, 2007), and sea surface temperatures near Iceland (Fig. 31) (Sicre et al., 2008) one can only wonder how a single tree-ring study could purport to prevail over such a huge amount of data. At best, if the tree-ring study did not accord with so much other data, it should simply mean that the tree rings were not sensitive to climate change, not that all the other data were wrong. McIntyre and McKittrick (2003, 2005) evaluated the data in the Mann paper and concluded that the Mann curve was invalid “*due to collation errors, unjustifiable truncation or extrapolation of source data, obsolete data, geographical location errors, incorrect calculation of principal components and other quality control defects*”. Thus, the “hockey stick” concept of global climate change is now widely considered totally invalid and an embarrassment to the IPCC.

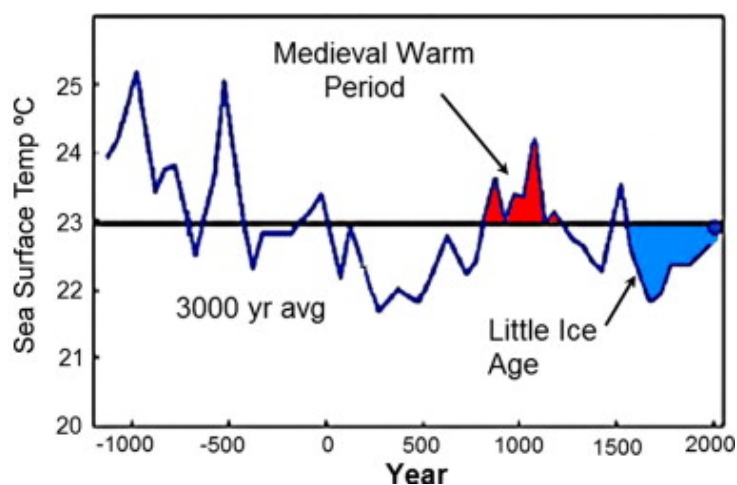


FIGURE 29. Surface temperatures of the Sargasso Sea reconstructed from isotope ratios in marine organisms (Keigwin, 1996).

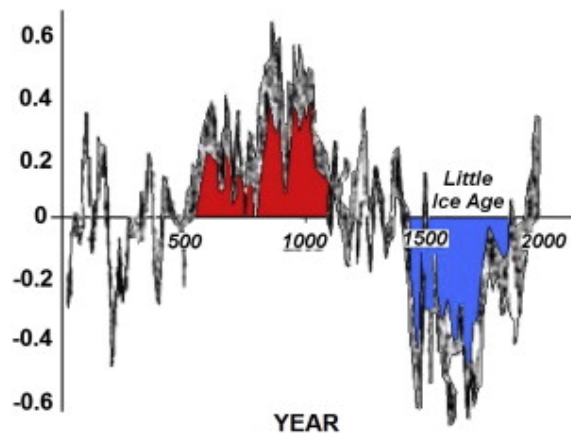


FIGURE 30. Reconstructed paleo-temperatures without tree ring data (Loehle, 2007).

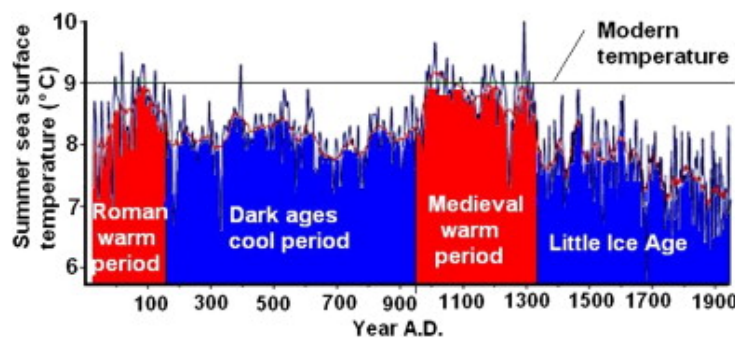


FIGURE 31. Summer sea surface temperatures near Iceland (Sicre et al., 2008).

Why, then, did Mann's hockey stick persuade so many non-scientists and gain such widespread circulation? The answer is apparent in revelations from e-mails disclosed in the Climategate scandal (Mosher and Fuller, 2010; Montford, 2010). These e-mails describe how they tried to “hide the decline” in temperatures, using various “tricks” in order to perpetuate a dogmatic view of anthropogenic global warming.

[> Read full chapter](#)

Temperature Fluctuations in Greenland and the Arctic

D.J. Easterbrook, in [Evidence-Based Climate Science \(Second Edition\)](#), 2016

1.1.7 Medieval Warm Period (900–1300 AD)

The [Medieval Warm Period](#) (MWP) was a time of warm climate from about 900–1300 AD, when global temperatures were somewhat warmer than at present. Temperatures in the GISP2 ice core were about 2°F (1°C) warmer than modern temperatures (Fig. 8.14). The effects of the warm period were particularly evident in Europe, where [grain crops](#) flourished, alpine tree lines rose, many new cities arose, and the population more than doubled.

The Vikings took advantage of the climatic [amelioration](#) to colonize southern Greenland in 985 AD, when milder climates allowed favorable open-ocean conditions for navigation and fishing. This was close to the maximum Medieval warming recorded in the GISP2 ice core at 975 AD (Stuiver et al., 1995). Erik the Red explored Greenland from Iceland and gave it its name. He claimed land in southern Greenland and became a chieftain about 985 AD. The first Greenlanders brought grain seed, probably barley, oats, and rye, horses, cattle, pigs, sheep, and goats. The southern coastal area was forested at the time. Greenland settlements lasted about 500 years before cooling during the [Little Ice Age](#) ended the settlements.

About 620 farms have been excavated in Greenland. Longhouses, the central residences of farm dwellers, would house 10 to 20 people who worked the farm. Ten persons per farm would put the population in Greenland at more than 6000 people, it but could have been as many as 8000–9000. From 1000 to 1300 AD the settlements thrived under a climate favorable to farming, trade, and exploration. A cooling, steadily deteriorating climate began after 1300 AD and farming became impractical. Three churches, one large estate, and 95 farms have been excavated on the west coast of Greenland, mostly under [permafrost](#). A bishop who travelled there about 1350 AD found that the settlement was completely abandoned. The Church abandoned Greenland in 1378 because ships could not get through the sea ice between Iceland and Greenland (Fig. 8.15).



Figure 8.15. Hvalsey Church, the place of the last recorded written record of the Norsemen in Greenland.

During the Medieval Warm Period, wine grapes were grown as far north as England, where growing grapes is now not feasible and about 300 miles (500 km) north of present [vineyards](#) in France and Germany. Grapes are presently grown in Germany up to elevations of about 1800 ft (560 m), but from about 1100 to 1300 AD, vineyards extended up to about 2500 ft (780 m), implying that temperatures were warmer by about 2–2.5°F (1–1.4°C). Wheat and oats were grown around Trondheim, Norway, suggesting that the climate was about 2°F (1°C) warmer than present (Fagan, 2007).

[> Read full chapter](#)

Using Patterns of Recurring Climate Cycles to Predict Future Climate Changes

D.J. Easterbrook, in [Evidence-Based Climate Science \(Second Edition\)](#), 2016

2.3.3 Medieval Warm Period (900–1300 AD)

The [Medieval Warm Period](#) (MWP) is the most contentious of the late [Holocene](#) climatic [oscillations](#) because of claims by the [Intergovernmental Panel on Climate Change](#) (IPCC) and CO₂ alarmists that it didn't really happen, ie, the basis for the infamous “hockey stick” assertion of no climate changes until CO₂ increase after 1950.

Oxygen [isotope](#) data from the GISP2 Greenland ice core clearly show a prominent MWP (Fig. 21.8) between 900 and 1300 AD. It was followed by global cooling and the beginning of the [Little Ice Age](#).

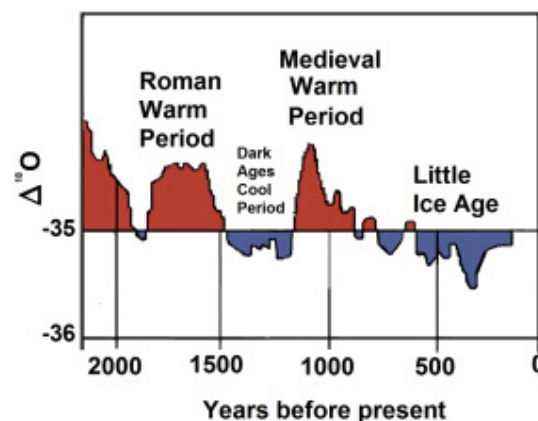


Figure 21.8. Oxygen isotope curve from the GISP2 Greenland ice core. (Red = warm, blue = cool.)

Plotted from *data* by Grootes, P.M., Stuiver, M., 1997. Oxygen 18/16 variability in Greenland snow and ice with 10₃ to 10₅-year time resolution. *Journal of Geophysical Research* 102, 26455–26470 data.

The MWP is also conspicuous on reconstruction of [sea surface temperature](#) near Iceland (Fig. 21.9; Sicre et al., 2008).

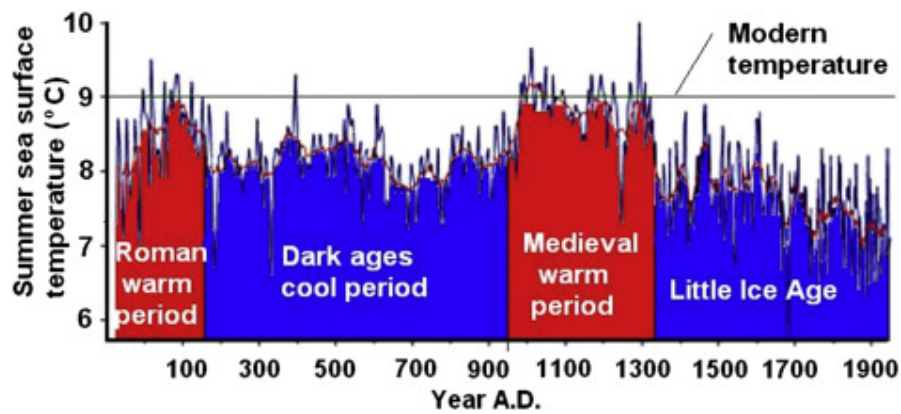


Figure 21.9. Summer sea surface temperatures near Iceland (Sicre et al., 2008).

As shown by numerous studies using a wide variety of methods, the MWP was a period of global warming. One example among many is the study of tree rings in China (Fig. 21.10; Liu et al., 2011).

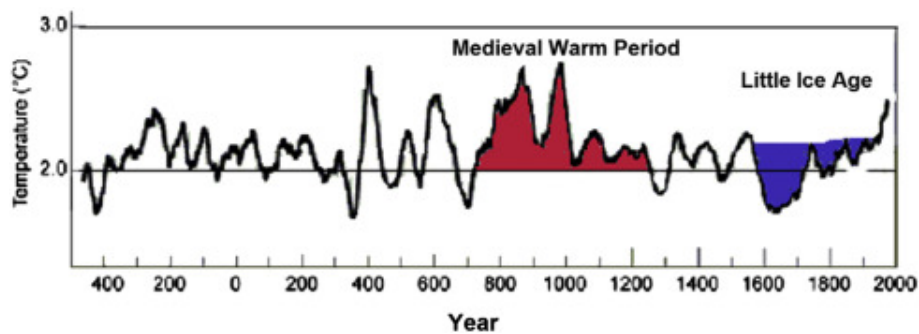


Figure 21.10. Temperature reconstruction from tree rings in China. (Red = warm, blue = cool.)

Modified from Liu, Y., Cai, Q.F., Song, H.M., et al., 2011. Amplitudes, rates, periodicities and causes of temperature variations in the past 2485 years and future trends over the central-eastern Tibetan Plateau. *Chinese Science Bulletin* 56, 2986–2994.

Historical accounts confirm the worldwide occurrence of the MWP. It was a time of warm climate from about 900 AD to 1300 AD. Its effects were evident in Europe, where [grain crops](#) flourished, alpine tree lines rose, many new cities arose, and the population more than doubled. The Vikings took advantage of the climatic [amelioration](#) to colonize Greenland, and wine grapes were grown as far north as England, where growing grapes is now not feasible, and about 500 km north of present [vineyards](#) in France and Germany. Grapes are presently grown in Germany up to elevations of about 560 m, but from about 1100 AD to 1300 AD., vineyards extended up to 780 m, implying temperatures warmer by about 1.0–1.4°C. Wheat and oats were grown around Trondheim, Norway, suggesting climates about 1°C warmer than present (Fagan, 2000).

Elsewhere in the world, prolonged [droughts](#) affected the southwestern United States and Alaska warmed. Sediments in central Japan record warmer temperatures. Sea surface temperatures in the Sargasso Sea were approximately 1°C warmer than

today (Keigwin, 1996), and the climate in equatorial east Africa was drier from 1000 AD to 1270 AD. An ice core from the eastern Antarctic [Peninsula](#) shows warmer temperatures during this period.

Oxygen isotope studies in Greenland, Ireland, Germany, Switzerland, Tibet, China, New Zealand, and elsewhere, plus tree-ring data from many sites around the world, all confirm the existence of a global MWP. Soon and Baliunas (2003) found that 92% of 112 studies showed physical evidence of the MWP, only 2 showed no evidence, and 21 of 22 studies in the [Southern Hemisphere](#) showed evidence of Medieval warming. Evidence of the MWP at specific sites is summarized in Fagan (2007) and Singer and Avery (2007).

Evidence that the MWP was a global event is so widespread that one wonders why Mann et al. (1998) ignored it. Over a period of many decades, several thousand papers were published establishing the MWP from about 900 AD to 1300 AD. Thus, it came as quite a surprise when Mann et al. (1998), on the basis of a single tree-ring study, concluded that neither the MWP nor the Little Ice Age actually happened and that assertion became the official position of the 2001 Intergovernmental Panel on Climate Change (IPCC). The IPCC 3rd report (Climate Change, 2001) totally ignored the several 1000 publications detailing the global climate changes during the MWP and the LIA and used the Mann et al. single tree-ring study as the basis for the now-famous assertion that “Our civilization has never experienced any environmental shift remotely similar to this. Today's climate pattern has existed throughout the entire history of human civilization” (Gore, 2007). This claim was used as the main evidence that increasing [atmospheric](#) CO₂ was causing global warming, and so, as revealed in the “Climategate” scandal, advocates of the CO₂ warming theory were very concerned about the strength of data showing that the MWP was warmer than the 20th century and had occurred naturally, long before atmospheric CO₂ began to increase. The Mann et al. “hockey stick” temperature curve was at so at odds with thousands of published papers, one can only wonder how a single tree-ring study could purport to prevail over such a huge amount of data.

McIntyre and McKittrick (2003) and McKittrick and McIntyre (2005) evaluated the data in the Mann paper and concluded that the Mann curve was invalid “due to collation errors, unjustifiable truncation or extrapolation of source data, obsolete data, geographical location errors, incorrect calculation of principal components and other quality control defects”. Thus, the “hockey stick” concept of global climate change is now widely considered totally invalid and an embarrassment to the IPCC.

[> Read full chapter](#)

A Critical Look at Surface Temperature Records

Joseph D'Aleo, in [Evidence-Based Climate Science](#), 2011

17 Long-Term Trends

Just as the [Medieval Warm Period](#) was an obstacle to those trying to suggest that today's temperature is exceptional, and the UN and its supporters tried to abolish it with the “hockey-stick” graph, the warmer temperatures in the 1930s and 1940s were another inconvenient fact that needed to be “fixed”.

In each of the databases, the land temperatures from that period were simply adjusted downward, making it look as though the rate of warming in the 20th century was higher than it was, and making it look as though today's temperatures were unprecedented in at least 150 years (Figs. 40–44).

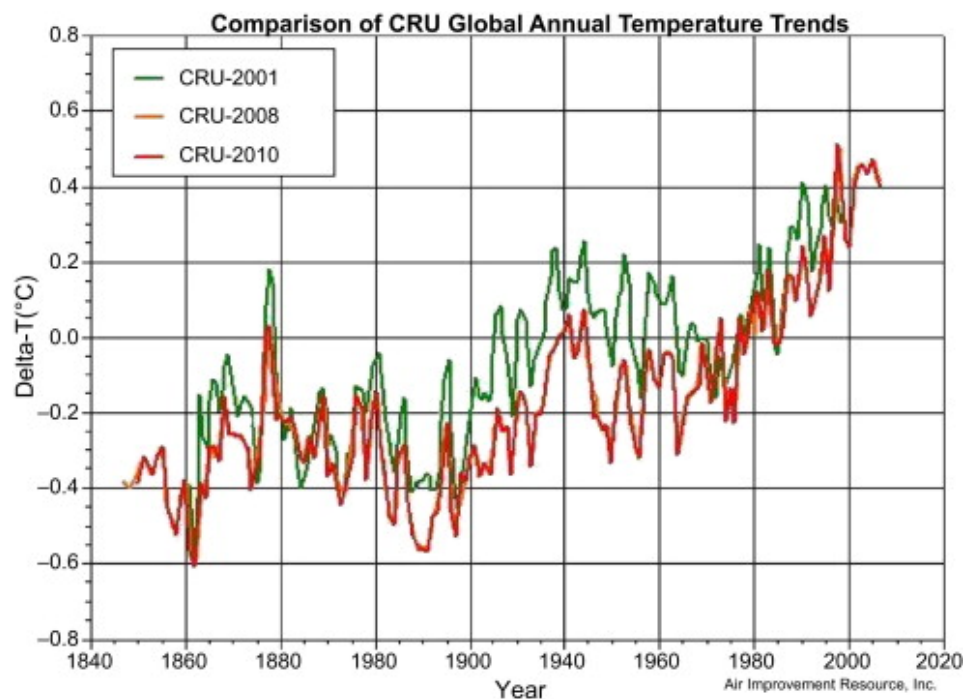


FIGURE 40. Comparing Hadley CRU 2001 vs. 2008 and 2010 annual mean temperatures.

GISS Temperatures Change Yearly				
	2006	2007	2008	2009
1996	-0.18	-0.16	-0.16	-0.06
1997	0.05	0.04	0.04	0.14
1998	1.24	1.24	1.24	1.31
1999	0.94	0.94	0.94	1.07
2000	0.65	0.54	0.54	0.69
2001	0.89	0.78	0.78	0.92
2002	0.67	0.55	0.55	0.69
2003	0.65	0.53	0.53	0.69
2004	0.54	0.46	0.46	0.61
2005	0.99	0.71	0.71	0.92
2006	*	1.15	1.15	1.31
2007	*	*	0.84	0.88
2008	*	*	*	0.12

FIGURE 41. Comparing NASA GISS values for recent years as reported in the year shown. Note the shift down in 2007 after correction for the millennium bug identified by McIntyre and then the shift up again in 2009.

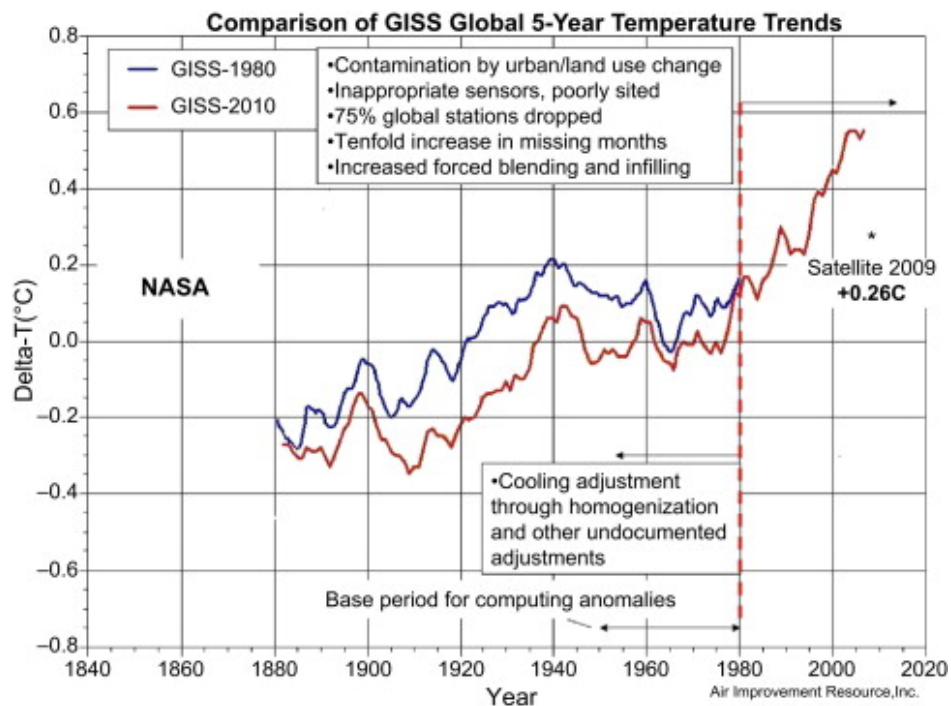


FIGURE 42. Comparing NASA GISS global values from 1980 to 2010. Note the string cooling prior to 1980. Warming post 1980 was due to many issues unaccounted for. Compare to UAH value for 2009.

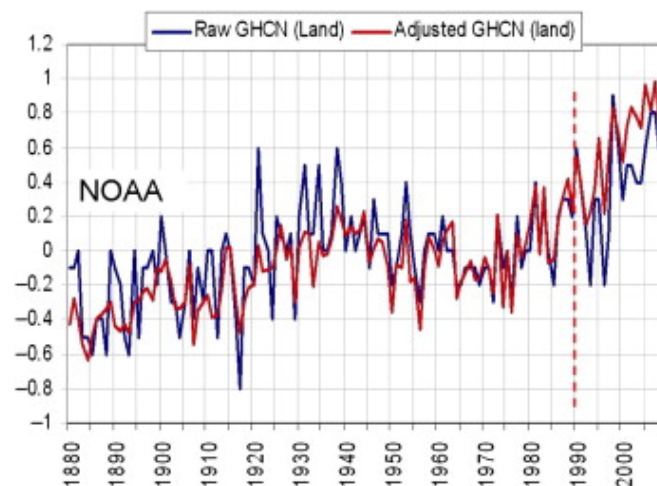


FIGURE 43. Comparing NOAA GHCN version 2 raw vs. adjusted. A similar cooling in the early record and recent warming is clearly shown. Raw data show little warming from peak in 1930s to 1940s to 1990s and 2000s.

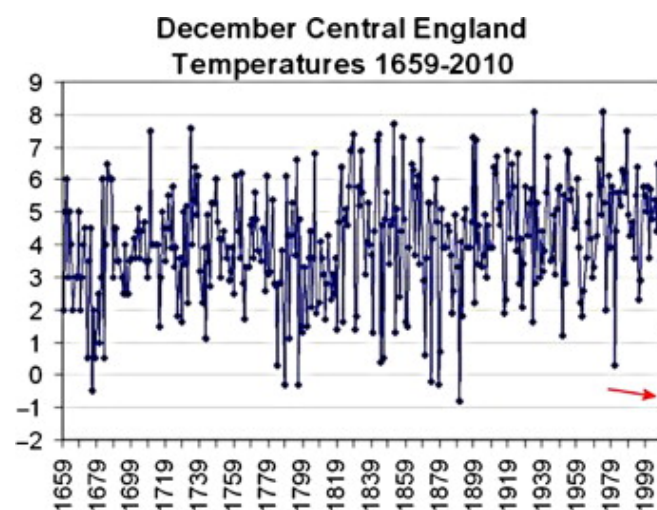


FIGURE 44. Central England Temperatures (CETs) for December from 1659 to 2010 second only 1890.

Wigley⁵⁸ even went so far as to suggest that [sea surface temperatures](#) for the period should likewise be “corrected” downward by 0.15C, making the 20th-century warming trend look greater but still plausible. This is obvious data doctoring.

In the Climategate emails, Wigley also noted⁵⁹:

“Land warming since 1980 has been twice the ocean warming — and skeptics might claim that this proves that urban warming is real and important.”

NOAA, then, is squarely in the frame. First, the unexplained major station [dropout](#) with a bias towards warmth in remaining stations. Next, the removal of the [urbanization](#) adjustment and lack of oversight and quality control in the siting of new instrumentation in the United States database degrades what once was the world's best data set, USHCNv1. Then, ignoring a large body of peer review research demonstrating the importance of urbanization and [land-use changes](#) NOAA chooses not to include any urban adjustment for the global data set, GHCN.

As shown, these and other changes that have been made alter the historical record and mask cyclical changes that could be readily explained by natural factors like multi-decadal ocean and solar changes.⁶⁰

The CRU data have seen changes even in the last decade with a cooling of the early and middle parts of the 20th century and dramatic post 1990 warming when most of the issues discussed emerged (Fig. 40).

The green is the 2001 global temperature plot and the red that in 2010 (with data through 2009).

Is NASA in the clear? No. It works with the same GHCN/USHCN base data (plus the SCAR data from Antarctica). To its credit, as we have shown its U.S. database includes an urban adjustment that is reasonable, but as Steve McIntyre showed⁶¹ uses NASA used population data and adjusted GHCN temperature records for cities in a warming direction as often as they do in a cooling direction. This we have seen is due to very poor [metadata](#) from GHCN which GISS uses to match with satellite night light to define a station as urban, suburban or rural.

And their [homogenization](#) process and other non-documented final adjustments result in an increase in apparent warming, often by cooling the early record as can be seen in several case studies that follow.

NASA also seems to constantly rehash the surface data. John Goetz⁶² showed that 20% of the historical record was **modified 16 times** in the 2½ years ending in 2007. 1998 and 1934 ping pong regularly between first and second warmest year as the fiddling with old data continues.

In 2007, NASA adjusted post-2000 data⁶³ when Steve McIntyre found a bug in the USHCN data down by 0.12 to 0.15C. Note how the data were adjusted up again in 2009 (USHCN V2.) (see Fig. 41)

Earlier version of NASA data was extracted from an earlier paper by Hansen in 1980 and is compared in the graph below. In 1987 (green on the graph in figure 42), the GISS temperatures were modified down in the middle part of the century from the 1980 version (blue) which enhanced the apparent warming in time for Dr. Hansen's testimony in front of congress.

Cooling before 1980 is dramatic. Warming after 1990 was due to the myriad of issues with the data in this period as we have identified above.

E-mail messages obtained by a [Freedom of Information](#) Act request reveal that NASA concluded that its own climate findings were inferior to those maintained by both the University of East Anglia's Climatic Research Unit (CRU) – the scandalized source of the leaked Climategate e-mails – and the National Oceanic and [Atmospheric](#) Administration's National Climatic Data Center.

The e-mails from 2007 reveal that when a *USA Today* reporter asked if NASA's data “was more accurate” than other climate-change data sets, NASA's Dr. Reto A. Ruedy replied with an unequivocal no. He said⁶⁴ “the National Climatic Data Center's procedure of only using the best stations is more accurate,” admitting that some of his own procedures led to less accurate readings.

“My recommendation to you is to continue using NCDC's data for the U.S. means and [East Anglia] data for the global means,” Ruedy told the reporter.

A similar tale is seen with NOAA GHCN version 2 before and after adjustment (Fig. 43).

The longest history of unaltered data is the Central England Temperature set established during the [Little Ice Age](#) in 1659. Note how this past December 2010 was the second coldest December in the record (just 0.1C above 1890). Long-term warming is seen coming out of the LIA but no acceleration upwards can be detected. (Fig. 44)

[> Read full chapter](#)

A Critical Look at Surface Temperature Records

J.S. D'Aleo, in [Evidence-Based Climate Science \(Second Edition\)](#), 2016

17 Long-Term Trends

Just as the [Medieval Warm Period](#) was an obstacle to those trying to suggest that today's temperature is exceptional, and the UN and its supporters tried to abolish it with the “hockey-stick” graph, the warmer temperatures in the 1930 and 1940s were another inconvenient fact that needed to be “fixed.”

In each of the databases, the land temperatures from that period were simply adjusted downward, making it look as though the rate of warming in the 20th century was higher than it was, and making it look as though today's temperatures were unprecedented in at least 150 years (Figs. 2.40–2.44).

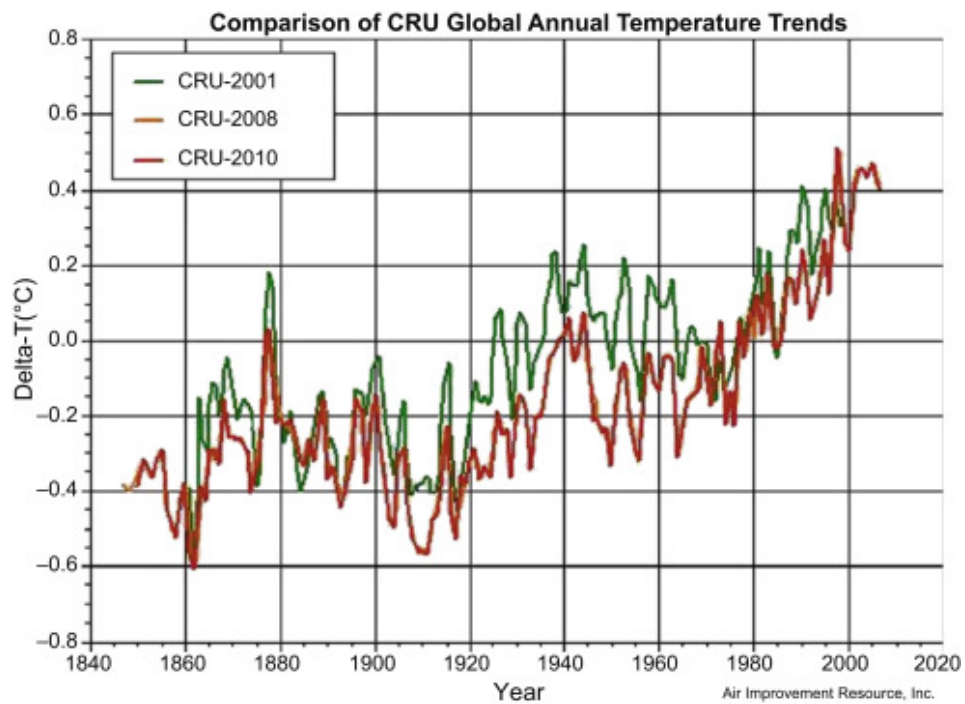


Figure 2.40. Comparing Hadley CRU 2001 versus 2008 and 2010 annual mean temperatures.

GISS Temperatures Change Yearly				
	2006	2007	2008	2009
1996	-0.18	-0.16	-0.16	-0.06
1997	0.05	0.04	0.04	0.14
1998	1.24	1.24	1.24	1.31
1999	0.94	0.94	0.94	1.07
2000	0.65	0.54	0.54	0.69
2001	0.89	0.78	0.78	0.92
2002	0.67	0.55	0.55	0.69
2003	0.65	0.53	0.53	0.69
2004	0.54	0.46	0.46	0.61
2005	0.99	0.71	0.71	0.92
2006	*	1.15	1.15	1.31
2007	*	*	0.84	0.88
2008	*	*	*	0.12

Figure 2.41. Comparing NASA GISS values for recent years as reported in the year shown. Note the shift down in 2007 after correction for the millennium bug identified by McIntyre and then the shift up again in 2009.

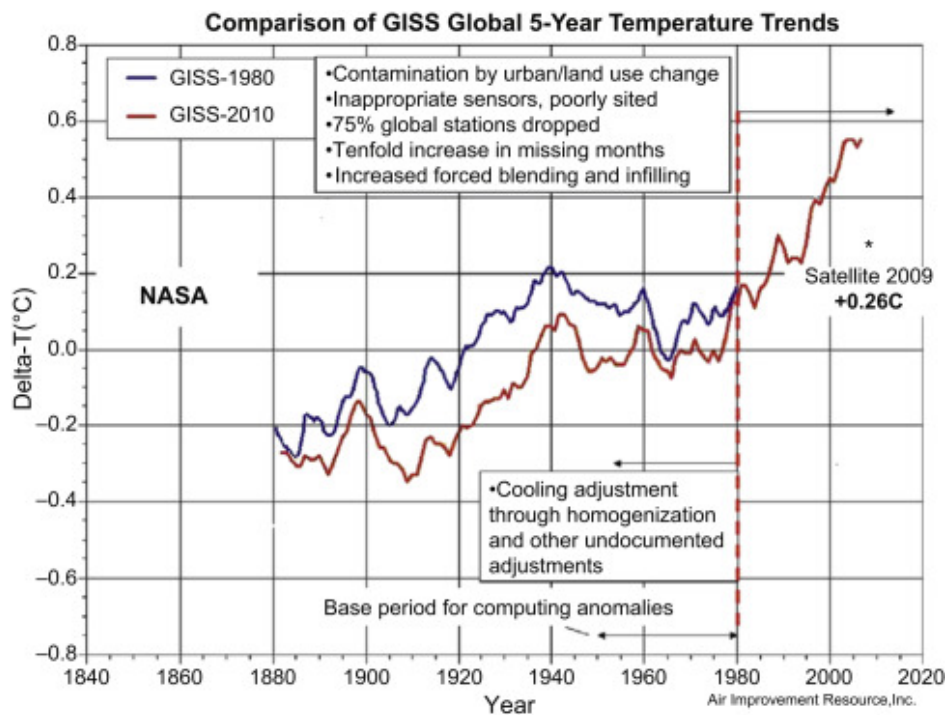


Figure 2.42. Comparing NASA GISS global values from 1980 to 2010. Note the string cooling prior to 1980. Warming post 1980 was due to many issues unaccounted for. Compare to UAH value for 2009.

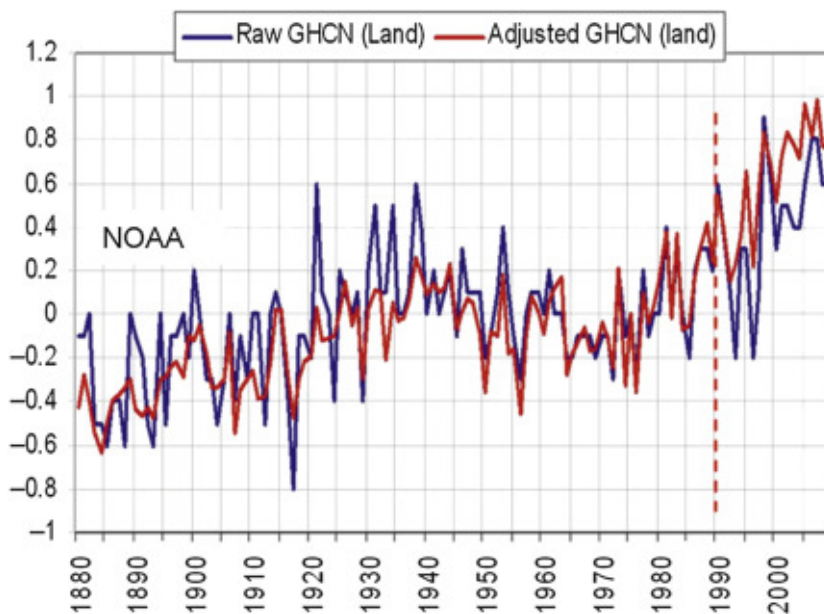


Figure 2.43. Comparing NOAA GHCN version 2 raw versus adjusted data. A similar cooling in the early record and recent warming is clearly shown. Raw data show little warming from peak in 1930s to 1940s to 1990s and 2000s.

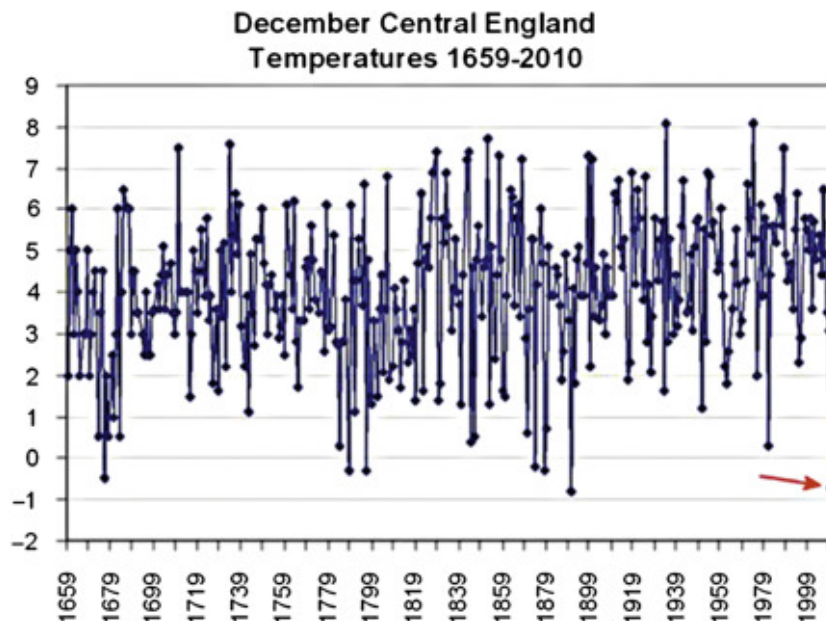


Figure 2.44. Central England Temperatures (CETs) for December from 1659 to 2010 s only 1890.

Wigley⁵⁸ even went so far as to suggest that [sea surface temperatures](#) for the period should likewise be “corrected” downward by 0.15°C, making the 20th-century warming trend look greater but still plausible. This is obvious data doctoring.

In the Climategate emails, Wigley also noted⁵⁹:

Land warming since 1980 has been twice the ocean warming—and skeptics might claim that this proves that urban warming is real and important.

NOAA, then, is squarely in the frame. First, the unexplained major station [dropout](#) with a bias towards warmth in remaining stations. Next, the removal of the [urban-ization](#) adjustment and lack of oversight and quality control in the siting of new instrumentation in the United States database degrades what once was the world's best data set, USHCNv1. Then, ignoring a large body of peer review research demonstrating the importance of urbanization and [land-use changes](#), NOAA chooses not to include any urban adjustment for the global data set, GHCN.

As shown, these and other changes that have been made alter the historical record and mask cyclical changes that could be readily explained by natural factors like multidecadal ocean and solar changes.⁶⁰

The CRU data have seen changes even in the last decade with a cooling of the early and middle parts of the twentieth century and dramatic post-1990 warming when most of the issues discussed emerged (Fig. 2.40). The green is the 2001 global temperature plot and the red that in 2010 (with data through 2009).

Is NASA in the clear? No. It works with the same GHCN/USHCN base data (plus the SCAR data from Antarctica). To its credit, as we have shown, its U.S. database includes an urban adjustment that is reasonable, but as Steve McIntyre showed,⁶¹ NASA uses

population data and adjusted GHCN temperature records for cities in a warming direction as often as they do in a cooling direction. This we have seen is due to very poor [metadata](#) from GHCN, which GISS uses to match with satellite night light to define a station as urban, suburban or rural.

And their [homogenization](#) process and other nondocumented final adjustments result in an increase in apparent warming, often by cooling the early record, as can be seen in several case studies that follow.

NASA also seems to constantly rehash the surface data. John Goetz⁶² showed that 20% of the historical record was **modified 16 times** in the 2½ years ending in 2007. 1998 and 1934 ping-pong regularly between first and second warmest year as the fiddling with old data continues.

In 2007, NASA adjusted post-2000 data,⁶³ when Steve McIntyre found a bug in the USHCN data, down by 0.12–0.15°C. Note how the data were adjusted up again in 2009 (USHCN V2) (see Fig. 2.41).

Earlier version of NASA data was extracted from an earlier paper by Hansen in 1980 and is compared in Fig. 2.42. In 1987 (green on the graph in Fig. 2.42), the GISS temperatures were modified down in the middle part of the century from the 1980 version (blue), which enhanced the apparent warming in time for Dr. Hansen's testimony in front of Congress.

Cooling before 1980 is dramatic. Warming after 1990 was due to the myriad of issues with the data in this period, as we have identified above.

E-mail messages obtained by a [Freedom of Information](#) Act request reveal that NASA concluded that its own climate findings were inferior to those maintained by both the University of East Anglia's CRU —the scandalized source of the leaked Climategate e-mails—and the National Oceanic and [Atmospheric](#) Administration's National Climatic Data Center.

The e-mails from 2007 reveal that when a *USA Today* reporter asked if NASA's data “was more accurate” than other climate-change data sets, NASA's Dr. Reto A. Ruedy replied with an unequivocal no. He said⁶⁴ “the National Climatic Data Center's procedure of only using the best stations is more accurate,” admitting that some of his own procedures led to less accurate readings.

“My recommendation to you is to continue using NCDC's data for the US means and [East Anglia] data for the global means,” Ruedy told the reporter.

A similar tale is seen with NOAA GHCN version 2 before and after adjustment (Fig. 2.43).

The longest history of unaltered data is the Central England Temperature set, established during the [Little Ice Age](#) in 1659. Note how December 2010 was the

second coldest December in the record (just 0.1°C above 1890). Long-term warming is seen coming out of the LIA but no acceleration upwards can be detected (Fig. 2.44).

[> Read full chapter](#)

Cause of Global Climate Changes

D.J. Easterbrook, in [Evidence-Based Climate Science \(Second Edition\)](#), 2016

1 Solar Variation—Grand Minima

At the end of the [Medieval Warm Period](#), ~1300 AD, temperatures dropped dramatically and the cold period that followed is known as the [Little Ice Age](#). The periods of colder climate that ensued for five centuries were devastating. The population of Europe had become dependent on [cereal](#) grains as a food supply during the Medieval Warm Period, and with the colder climate, early snows, violent storms, and recurrent flooding that swept Europe, massive crop failures occurred, resulting in widespread [famine](#) and disease (Fagan, 2000; Grove, 2004). Glaciers in Greenland and elsewhere began advancing and pack ice extended southward in the North Atlantic, blocking ports and affecting fishing. Three years of torrential rains that began in 1315 led to the Great Famine of 1315–1317.

The Little Ice Age was not a time of continuous cold climate, but rather repeated periods of cooling and warming, each of which occurred during times of solar minima, characterized by low [sunspot](#) numbers, low total solar [irradiance](#) (TSI), decreased solar [magnetism](#), increased cosmic ray intensity, and increased production of radiocarbon and [beryllium](#) in the upper atmosphere.

Centuries of observations of the sun have shown that [sunspots](#), solar irradiance, and solar magnetism vary over time, and these phenomena correlate very well with global climate changes on Earth. A number of solar Grand Minima, periods of reduced solar output, have been recognized (Fig. 14.1).

Selected solar activity events

Event	Approx dates	
Medieval maximum	1100	1250
Wolf minimum	1280	1350
Spörer Minimum	1460	1550
Maunder Minimum	1645	1715
Dalton Minimum	1790	1820
1880-1915 Minimum	1880	1915
1945-1977 Minimum	1945	1977

Figure 14.1. Solar minima.

1.1 Wolf Minimum (1290–1320 AD)

The Wolf Minimum was a period of low sunspot numbers (SSNs) and TSI between about 1300 and 1320 AD. It occurred during the cold period that marked the end of the Medieval Warm Period (MWP) and the beginning of the Little Ice Age (LIA) about 1300 AD.

The change from the warmth of the MWP to the cold of the LIA was abrupt and devastating, leading to the Great Famine from 1310 to 1322. The winter of 1309–1310 AD was exceptionally cold. The Thames River froze over and poor people were especially affected. The year 1315 AD was especially bad. Jean Desnouelles wrote at the time, “Exceedingly great rains descended from the heavens and they made huge and deep mud-pools on the land. Throughout nearly all of May, June, and August, the rains did not stop.” Corn, oats, and hay crops were beaten to the ground, August and September were cold, and floods swept away entire villages. Crop harvests in 1315 AD were a disaster, affecting an enormous area in northern Europe. In places, up to half of [farmlands](#) were eroded away, cold, wet weather prevented grain harvests, and fall plantings failed, triggering famines.

In 1316 AD, spring rain continued, again impeding the sowing of grain crops, and harvests failed once again. Diseases increased, newborn and old people died of [starvation](#), and multitudes scavenged anything edible. Whole communities disappeared and many farms were abandoned. The year 1316 was the worst for [cereal crops](#) in the entire [Middle Ages](#). Cattle couldn’t be fed, hay wouldn’t dry and couldn’t be moved so it just rotted. Thousands of cattle froze during the bitterly cold winter of 1317–1318 and many others starved. The cold immobilized shipping. Rain in 1317–1318 continued through the summer and people suffered for another seven years. The coincidence of sudden cooling of the climate from the warm Medieval Warm Period to the harsh cold climate of the Little Ice Age during the Wolf Minimum was not just a coincidence, as shown by at least five later, similar instances.

1.2 Sporer Minimum (1410–1540)

The Sporer Minimum occurred from about 1410 to 1540 (Fig. 14.1). Like the Wolf Minimum, the Sporer coincided with a cold period (Fig. 14.2).

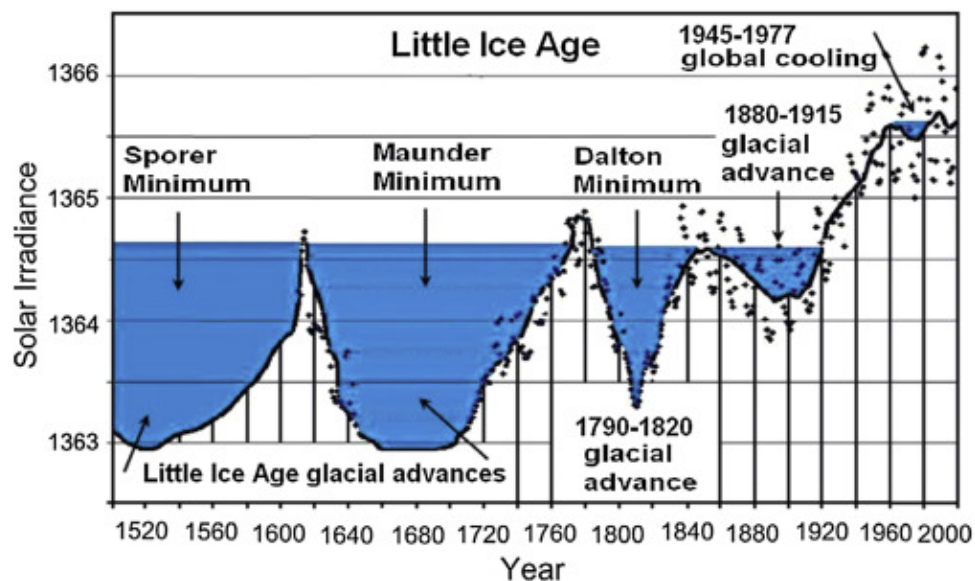


Figure 14.2. Relationship of solar minima, solar irradiance, and glacier advances. Blue areas were cool periods. Cool climates prevailed in all six solar minima since 1300 AD.

1.3 Maunder Minimum

The [Maunder Minimum](#) is the most famous cold period of the Little Ice Age. Temperatures plummeted in Europe (Figs. 14.3–14.7), the growing season became shorter by more than a month, the number of snowy days increased from a few to 20–30, the ground froze to several feet, alpine glaciers advanced all over the world, glaciers in the Swiss Alps encroached on farms and buried villages, tree-lines in the Alps dropped, sea ports were blocked by sea ice that surrounded Iceland and Holland for about 20 miles, wine grape harvests diminished, and cereal grain harvests failed, leading to mass famines (Fagan, 2007). The Thames River and canals and rivers of the Netherlands froze over during the winter (Fig. 14.3). The population of Iceland decreased by about half. In parts of China, warm-weather crops that had been grown for centuries were abandoned. In North America, early European settlers experienced exceptionally severe winters.



Figure 14.3. 1663 painting by Jan Grifier of the frozen Thames River in London during the Maunder Minimum.



Figure 14.4. Glaciers in the Alps advanced during the Little Ice Age.

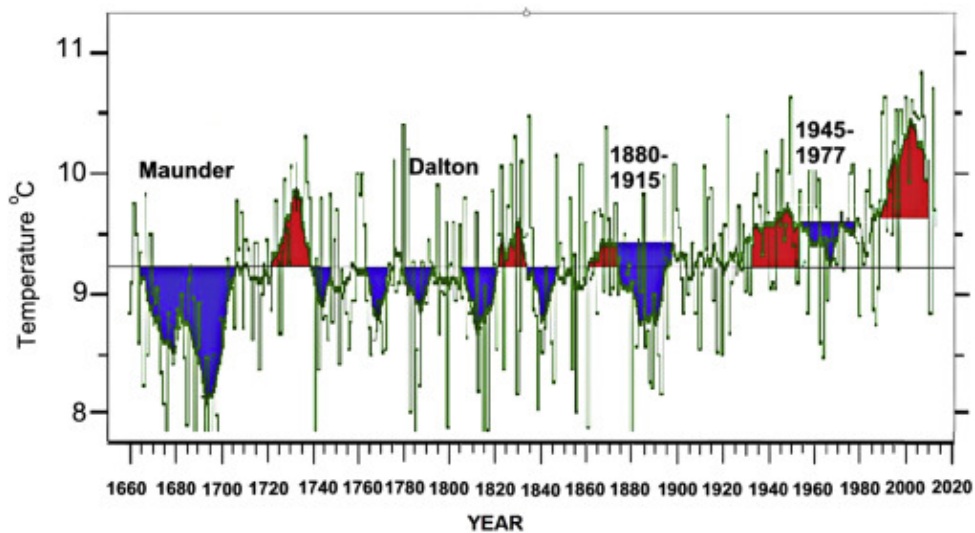


Figure 14.5. Central England temperatures (CET) recorded continuously since 1658. Blue areas are reoccurring cool periods; red areas are warm periods. All times of solar minima were coincident with cool periods in central England.

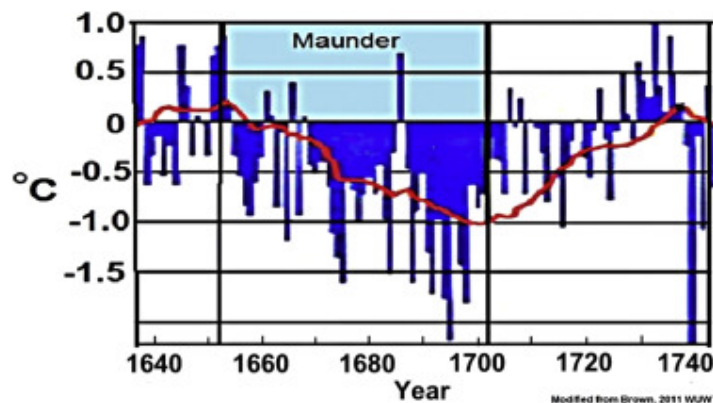


Figure 14.6. CET during the Maunder Minimum.

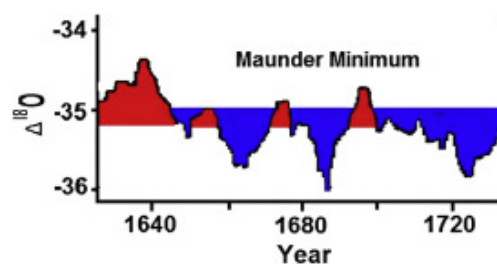


Figure 14.7. Oxygen isotope record, GISP2 Greenland ice core showing the Maunder Minimum. Blue area is cool, red is warm. The isotope record shows the same cooling as the CET.

1.3.1 Sunspots

Sunspots are temporary dark spots on the surface of the sun (Fig. 14.8), where concentrations of magnetic field flux inhibit convection, reducing surface temperature. They occur in pairs and may last from a few days to a few months before eventually disappearing. Sunspots expand and contract as they move across the surface of the sun, ranging from 16 km (10 mi) to 160,000 km (100,000 mi) in diameter. Sunspots

usually appear in groups. Sunspot activity cycles about every 11 years. The point of highest sunspot activity during a cycle is known as solar maximum, and the point of lowest activity as solar minimum.

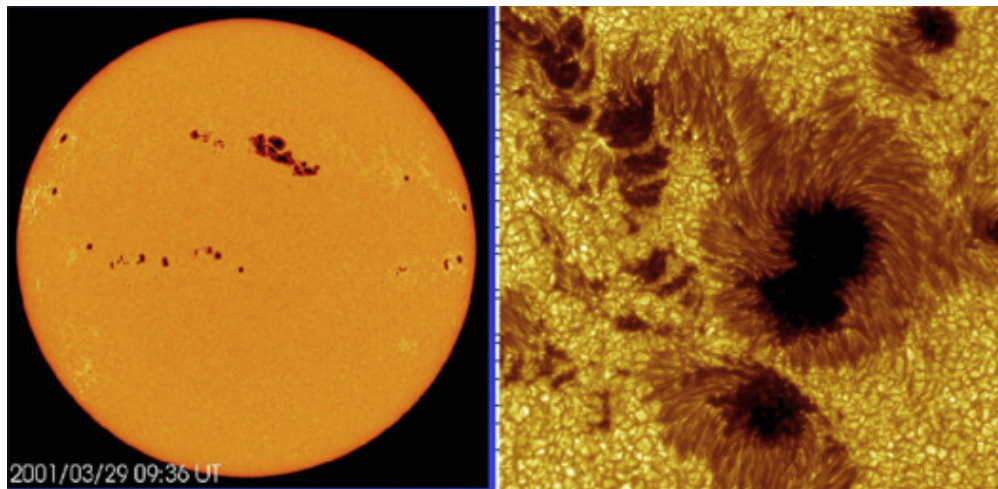


Figure 14.8. Sunspots.

NASA images.

When Galileo perfected the telescope in 1609, scientists could see sunspots for the first time. They were of such interest that records were kept of the number of sunspots observed, and although not perfectly accurate due to cloudy days, lost records, and so on, the records show a remarkable pattern for more than a century (Fig. 14.9) (Maunder, 1894, 1922; Eddy, 1976, 1977; Soon, 2005; Hoyt and Schatten, 1997, 1998; Lean et al., 1995, 2002). From 1600 to 1715 AD, very few sunspots were seen, and from 1645 to 1715, many years had no sunspots at all, despite the fact that many scientists with telescopes were actively looking for them. The longest known minimum (about 50 years) of virtually no sunspots occurred during the Maunder Minimum. After 1715 AD, the number of observed sunspots increased sharply from near zero to 50–100 (Fig. 14.9) and the global climate warmed.

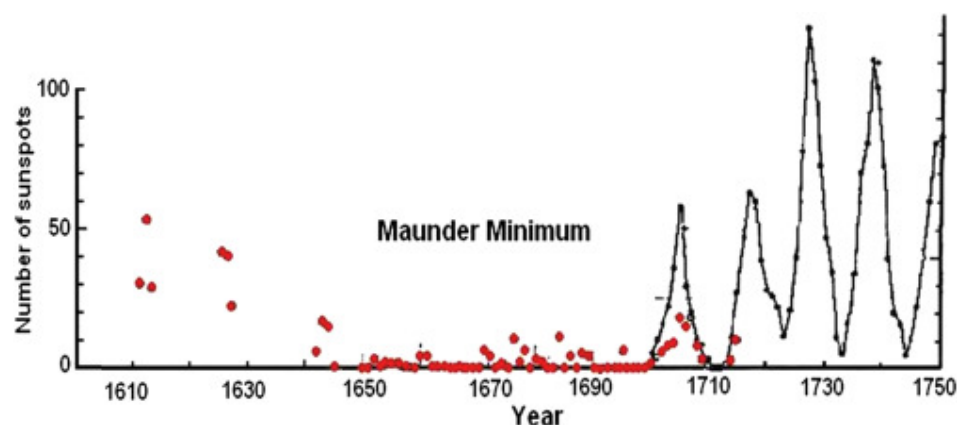


Figure 14.9. Sunspots during the Maunder Minimum. From 1645 to 1700, many years had no sunspots.

1.3.2 Total Solar Irradiance

TSI is the solar radiative power per unit area incident on the Earth's upper atmosphere. It is usually measured in watts per square meter (W/m^2). It has varied historically, reaching maximums during periods of high sunspot numbers and minimums during of low sunspot numbers (Fig. 14.10). TSI drops to lowest values during Solar Minimums and during sunspots lows.

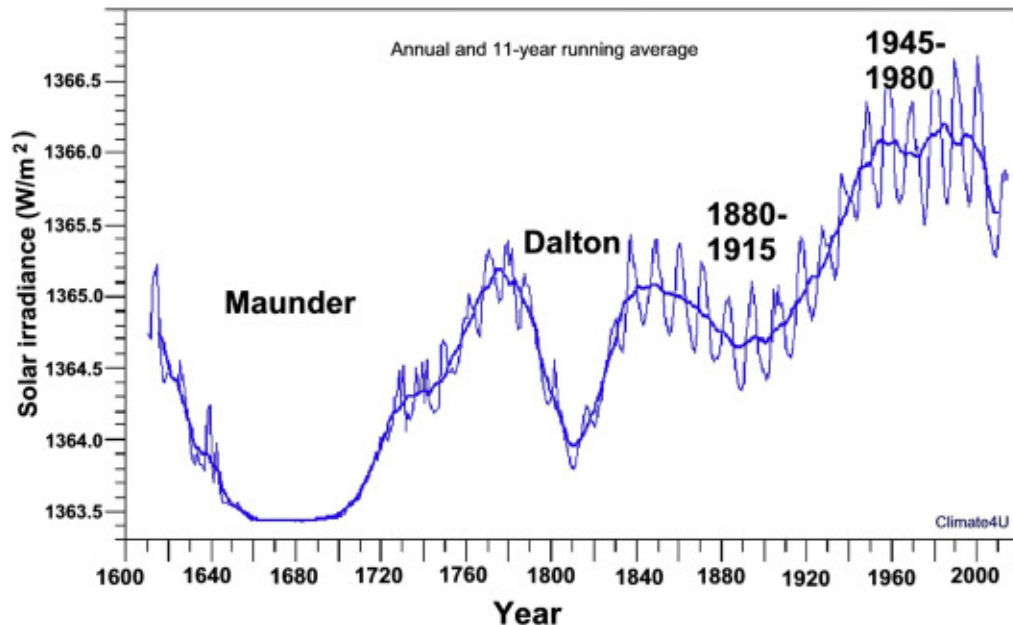


Figure 14.10. Total solar irradiance from 1600 to 2014 AD.

Modified from Lean, J.L., Beer, J., Bradley, R., 1995, Reconstruction of solar irradiance since 1610: implications for climatic change. *Geophysics Research Letters* 22, 3195–3198.

1.3.3 Temperature, Sunspots, and Total Solar Irradiance

Temperatures during the Maunder closely correlate with SSNs and TSI (Fig. 14.11). When SSNs and TSI are low, temperatures are also low, and when SSNs and TSI are high, temperatures are high.

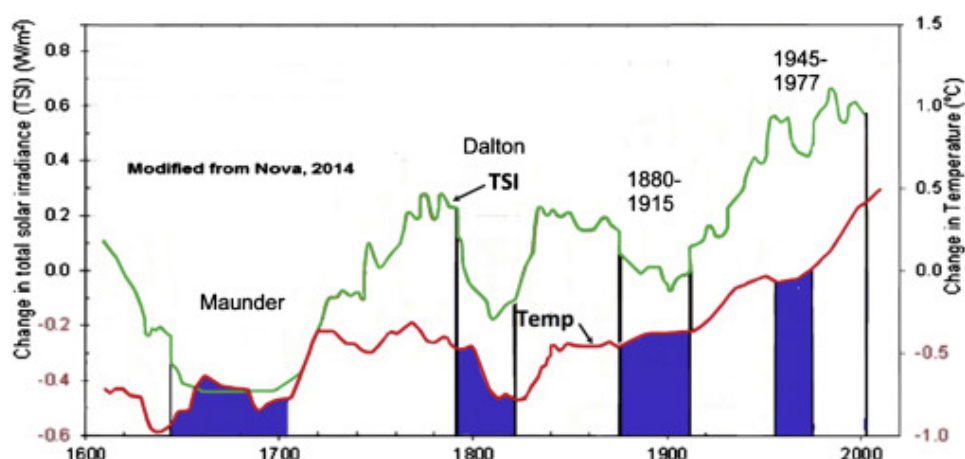


Figure 14.11. Correlation of total solar irradiance (TSI) and temperature.

Modified from Nova, 2014.

1.4 Dalton Minimum

The Dalton Minimum was a period of low SSNs and TSI from about 1790 to 1820. Like the Maunder, it was a time of intense cooling and great hardship, although not as bad as the Maunder. Widespread famines due to crop failures spread across Europe. Several notable events occurred during the Dalton, including the French Revolution and Napoleon's defeat in Russia because of a bitterly cold winter.

The cool temperatures of the Dalton show up both in the CET and GISP2 Greenland ice core (Figs. 14.12 and 14.13).

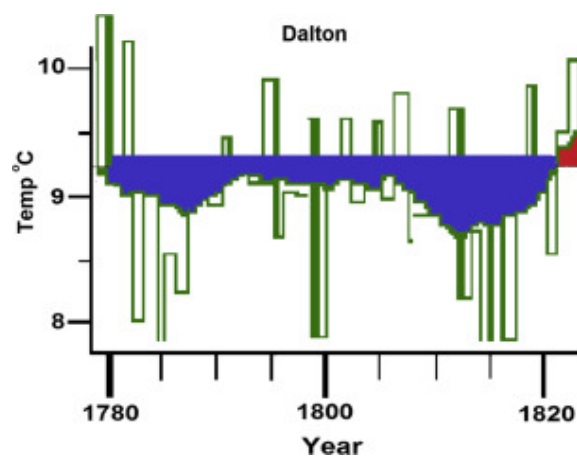


Figure 14.12. CET during the Dalton Minimum.

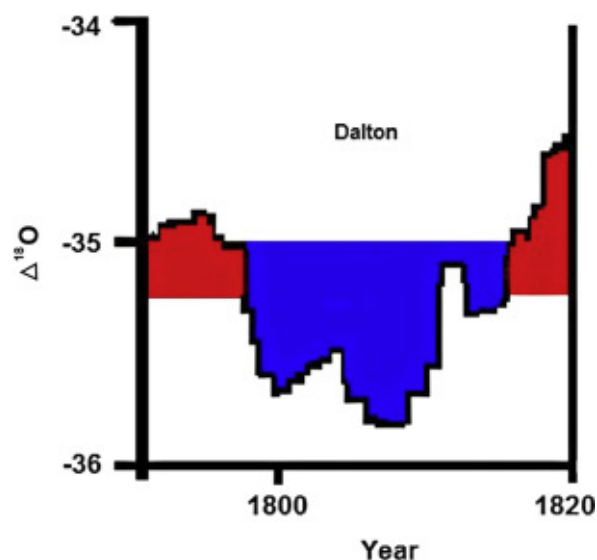


Figure 14.13. Oxygen isotope record from the GISP2 Greenland ice core.

Data from Grootes and Stuiver.

1.4.1 Sunspots

Sunspots declined sharply during the Dalton Minimum (Fig. 14.14).



Figure 14.14. Sunspots during the Dalton Minimum.

Plotted from Svalgaard data.

1.4.2 Total Solar Irradiance

TSI also declined sharply during the Dalton Minimum (Fig. 14.10).

1.4.3 Temperature and Total Solar Irradiance

During the Dalton Minimum, temperatures dropped, closely following TSI (- Fig. 14.15).

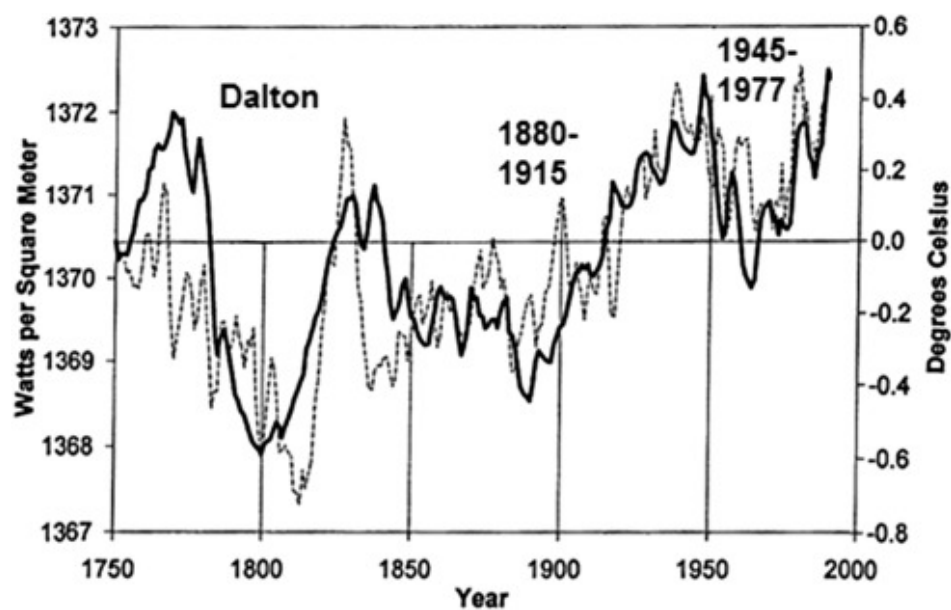


Figure 14.15. Solar irradiance and global temperature from 1750 to 1990. During this 250-year period, temperature and total solar irradiance curves follow a remarkably similar pattern.

Modified from Hoyt, D.V., Schatten, K.H., 1997, *The Role of the Sun in Climate Change*: Oxford University, p. 279.

1.5 1880–1915 Minimum

Temperatures dropped sharply beginning about 1880, and the 1850–1880 warm period came to a close and the climate cooled (Figs. 14.16–14.18). Alpine glaciers advanced down valley to terminal positions not far from their maximums during the early part of the LIA.

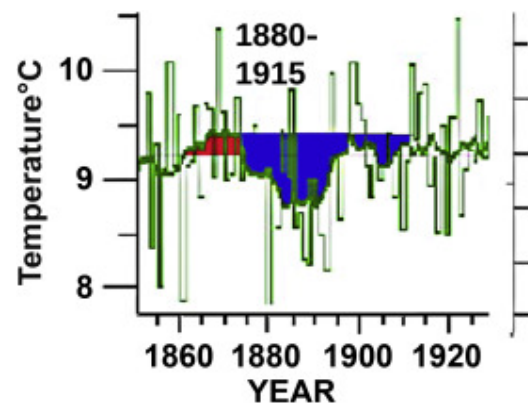


Figure 14.16. CET during the 1880–1915 cool period.

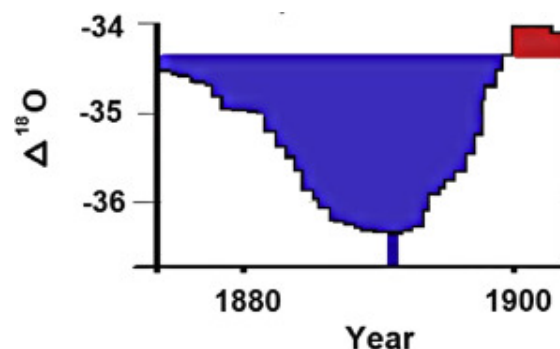


Figure 14.17. Oxygen isotope record from the GISP2 Greenland ice core. Blue area is cool.

Data from Grootes, P.M., Stuiver, M., 1997. Oxygen 18/16 variability in Greenland snow and ice with 10³ to 10⁵-year time resolution: *Journal of Geophysical Research* 102, 26455–26470.

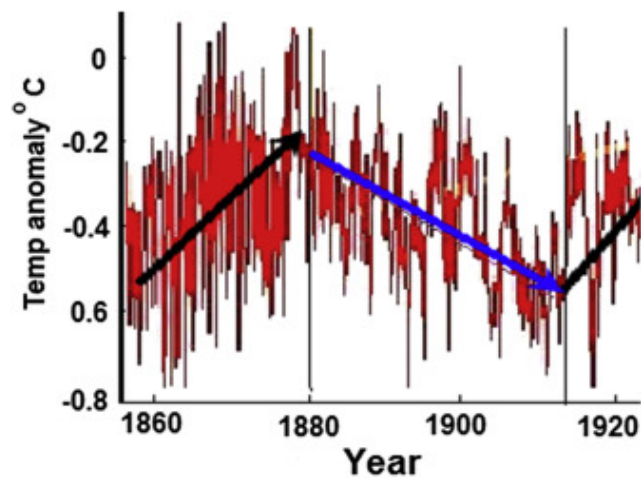


Figure 14.18. Global temperature, 1880 to 1915 cool period.

Modified from HADRUT3.

1.5.1 Sunspots

The number of sunspots declined during the 1880–1915 cool period (Fig. 14.19).

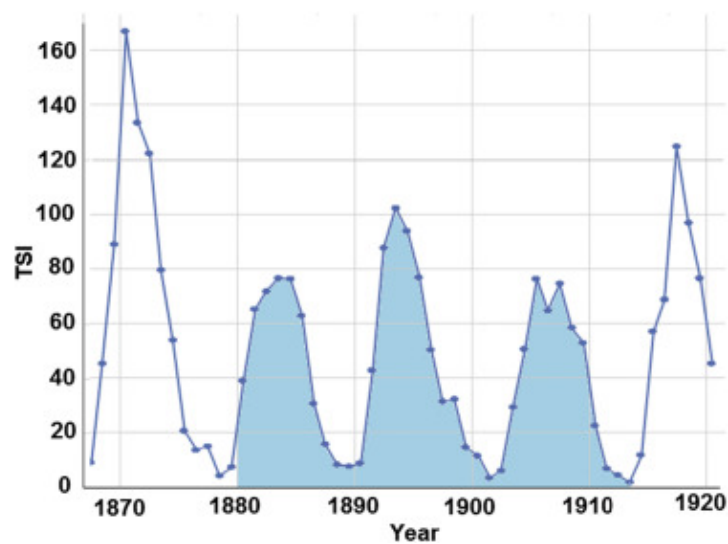


Figure 14.19. Sunspots during the 1880–1915 cool period.

1.5.2 Total Solar Irradiance and Temperature

TSI declined during the 1880–1915 cool period (Fig. 14.10). Temperature closely followed TSI (Fig. 14.20).

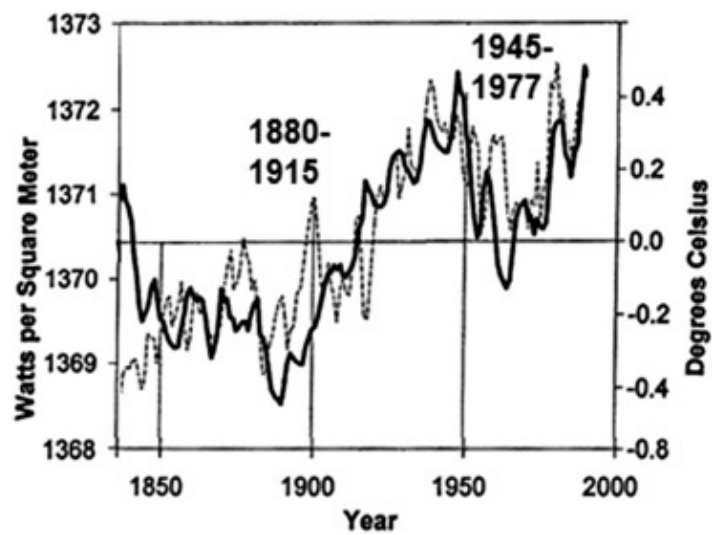


Figure 14.20. Total solar irradiance and temperature during the 1880–1915 cool period.

1.6 1945–1977 Minimum

Following the early 20th-century warm period (1915–1945), the climate cooled for 30 years (Figs. 14.21 and 14.22).

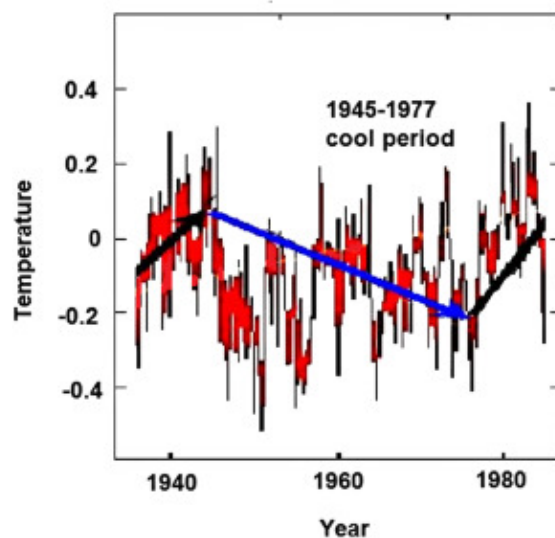


Figure 14.21. Temperature during the 1945–1977 cool period.

HADCRUT3.

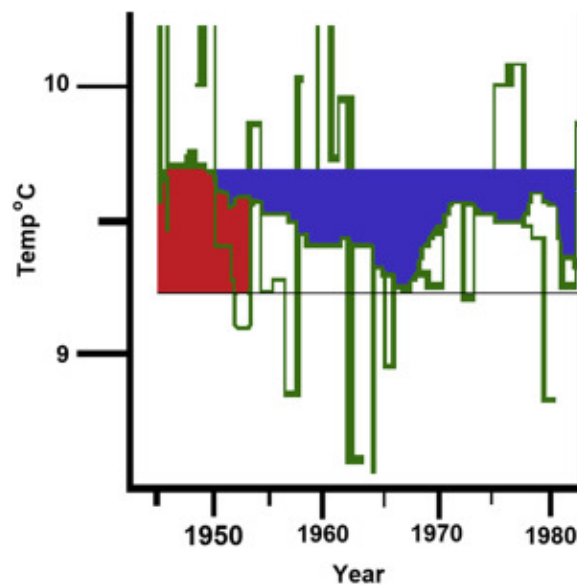


Figure 14.22. CET during the 1945–1977 cool period. (Blue = cool, red = warm.)

1.6.1 Sunspots

The number of sunspots declined during the 1945–1977 cool period (Fig. 14.23).

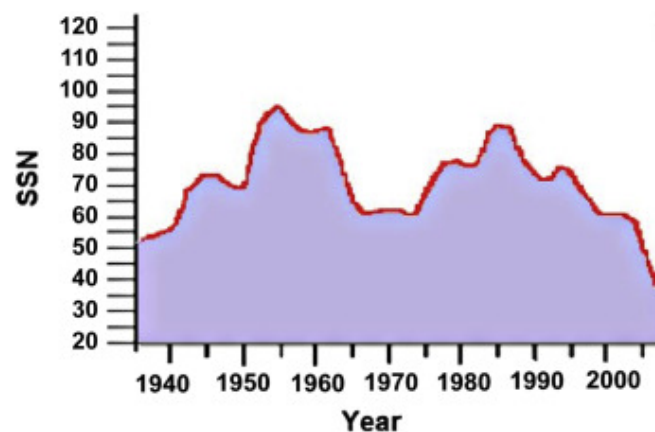


Figure 14.23. SSNs during the 1945–1977 cool period.

1.6.2 Total Solar Irradiance and Temperature

Decline in TSI coincided with 30 years of global cooling temperatures from 1945 to 1977 (Fig. 14.20), even as CO₂ emissions soared.

[> Read full chapter](#)

Lake Bonneville

R.S. Thompson, ... J.P. McGeehin, in [Developments in Earth Surface Processes](#), 2016

11.6.8 Late Holocene: The Last 2000 Years

Many paleoclimatic studies of the last 2000 years frame their results in terms of commonly employed terms such as the [Medieval warm period](#) and LIA. Regrettably, as discussed in Jones and Mann (2004) this practice can mask much of the variability seen through this time period, and an unfortunate human tendency exists to see what we already believe in our proxy records. In western North America, glaciers continued to advance and retreat through the last 2000 years (see Munroe et al. (2012) for a detailed discussion), with prominent periods of [glaciation](#) ~ 1.7 to ~ 1.3 cal ka (“the First Millennium” glaciation, FM) and ~ 0.7 to ~ 0.1 cal ka (the more extensive “LIA”). Within the Great Basin during this time, both sustained periods occurred of relatively high effective moisture (such as those associated with higher-than-historical lake levels in western Nevada from ~ 1.5 to ~ 1.3 cal ka and ~ 0.9 to ~ 0.7 cal ka; Adams, 2003), as well as major periods of [drought](#) (such as those identified by Mensing et al., 2008, as ending ~ 1.8, ~ 1.2, ~ 0.8, and ~ 0.6 cal ka). See Wigand (2006) and Grayson (2011) for more detailed discussions of the complexities of the last 2000 years of paleoclimatic variability in the Great Basin [region](#).

After the period of cooler and moister conditions during the 2000 years of GSL96 + subzone E2, the succeeding (and final) subzone (E3) presents a more complex picture with considerably more apparent variability. The increased variability may in part be an artifact: we sampled the core at a relatively coarse interval of depth (7 to 9 cm on average across the three subzones of [pollen zone E](#)), and since the [accumulation rate](#) is much faster in E3 (and/or the sediments are less compacted) than in the lower subzones, the average temporal spacing between samples varies from ~ 139 years for E1, ~ 146 years for E2, and ~ 66 years for E3. Consequently, the greater variability in E3 may simply be a reflection of its higher sampling resolution.

Within pollen subzone E3, two episodes (~ 1.8 to 1.7 cal ka and ~ 0.6 to ~ 0.2 cal ka) occur of sustained high levels of *Juniperus* pollen that we interpret as representing relatively cool and/or wet climatic conditions. These episodes appear to align temporally with the FM and LIA glacial episodes, and fall outside of the drought periods identified by Mensing et al. (2008). [Pollen](#) spectra from the period between the *Juniperus* peaks have lower percentages of *Juniperus* and relatively high levels of *Amaranthaceae*, which together suggest relatively dry conditions. At the top of E3, *Juniperus* declines to its lowest levels in the subzone and *Artemisia* reaches its highest levels for pollen zone E overall. These changes can plausibly be due to warmer and drier conditions following the LIA, but may also reflect intensifying land use over the past century.

In general, vegetation represented by packrat [middens](#) dated to within the last 2 cal ka resembles the present-day native vegetation at the [midden](#) localities (Rhode,

2000b), although some middens contain *Juniperus* below its modern lower limits (Rhode, 2000b; Madsen et al., 2001). It appears that the lower limit of this taxon fluctuated through subzone E3 time, but it is not possible to align the high E3 *Juniperus* pollen episodes with the midden records. In addition, fish remains from Homestead Cave suggest a rise of GSL at ~ 1.1 cal ka (Madsen et al., 2001), which also falls outside of the high *Juniperus* episodes in subzone E3.

Many of the published pollen records in the Bonneville basin and surrounding region have low sampling resolution for the last 2000 years, and they also do not present a unified picture on paleoclimatic changes over this time. For example, the record from Swan Lake (Bright, 1966) has higher percentages of *Artemisia* and lower percentages of conifer pollen than earlier, suggesting warmer conditions than during the preceding 2000 years (and this is roughly similar to the differences between GSL96 + subzones E2 and E3). In contrast, the nearby Grays Lake pollen record (Beiswenger, 1991) has higher percentages of the pollen of montane conifers in the last 2000 years, and lower representation of *Juniperus* and *steppe* taxa, which seem to give the opposite signal to the Swan Lake record.

For the last 2000 years at Mission Cross *Bog*, Thompson (1984) found increased *Pinus* and *Ceanothus* and the lowest values in the record of *Amaranthaceae*, *Juniperus*, and *Poaceae*, with the interpretation that conditions were warmer than those of 4 to 2 cal ka, but cooler/wetter than prior to ~ 4.7 cal ka. A higher resolution study of the past 4 ka in this bog (Allan, 2003; Mensing et al., 2008) also found that the period from ~ 2 cal ka to the present was generally drier than, and had more extended droughts than, the prior 2000 years. The opposite interpretation was made for the Ruby *Marshes* (Thompson, 1992) where higher values of *Artemisia* relative to *Amaranthaceae*, together with apparently deeper waters, suggested cool and moist conditions over the past 500 years. Yet another pattern was identified at Favre Lake, where Wahl et al. (2015) found the last ~ 1.8 cal ka of the record to be more variable and wetter than earlier, but with lower lake levels occurring between ~ 1.0 and 0.75 cal ka.

In the Snake Range, the chironomid-based reconstruction from Stella Lake has relatively cold summer temperatures until ~ 1.6 cal ka, with the coldest temperatures occurring between ~ 1.8 and ~ 1.6 cal ka. Following this episode, a warming trend occurs, with the exception of a cold excursion at ~ 1.2 cal ka (Reinemann et al., 2009). At higher elevations of the Snake Range, LaMarche and Mooney (1972) found no evidence of higher-than-present upper treelines over the past 2000 years. However, in the White Mountains of California, treelines remained above present levels until ~ 0.9 cal ka and then declined to at least modern levels by ~ 0.5 cal ka (LaMarche, 1973). Similarly, in Colorado, higher-than-present upper treelines were present from prior to 2 cal ka until ~ 0.8 cal ka (Carrara and McGeehin, 2015).

To summarize, most paleoclimatic studies in and near the Bonneville basin are in agreement that the last 2000 years have been generally warmer and drier, and probably more variable, than the preceding 2000 years. The sequence of paleoclimatic changes that we interpret from pollen subzone E3 is commensurate with the pattern of glacial advances and retreats seen in the North America [Cordillera](#) and with the broad narrative of change for the [Northern Hemisphere](#) for the past 2000 years. However, it is difficult to make any detailed comparisons within the Bonneville basin region, given limitations of chronological controls, sampling resolutions, and apparently differing sensitivities and rates of responses for the various paleoclimatic proxy data.

[> Read full chapter](#)

Holocene Climate Variability*

M. Maslin, ... V. Ettwein, in [Encyclopedia of Ocean Sciences \(Second Edition\)](#), 2001

Little Ice Age (LIA)

The most recent [Holocene](#) cold event is the [Little Ice Age](#) (see Figures 2 and 3). This event really consists of two cold periods, the first of which followed the [Medieval Warm Period](#) (MWP) that ended \sim 1000 years ago. This first cold period is often referred to as the Medieval Cold Period (MCP) or LIAb. The MCP played a role in extinguishing Norse colonies on Greenland and caused [famine](#) and mass migration in Europe. It started gradually before ad 1200 and ended at about ad 1650. This second cold period, may have been the most rapid and the largest change in the North Atlantic during the Holocene, as suggested from ice-core and deep-sea [sediment](#) records. The Little Ice Age events are characterized by a drop in temperature of 0.5–1°C in Greenland and a [sea surface temperature](#) falls of 4°C off the coast of west Africa and 2°C off the Bermuda Rise (see Figure 3).

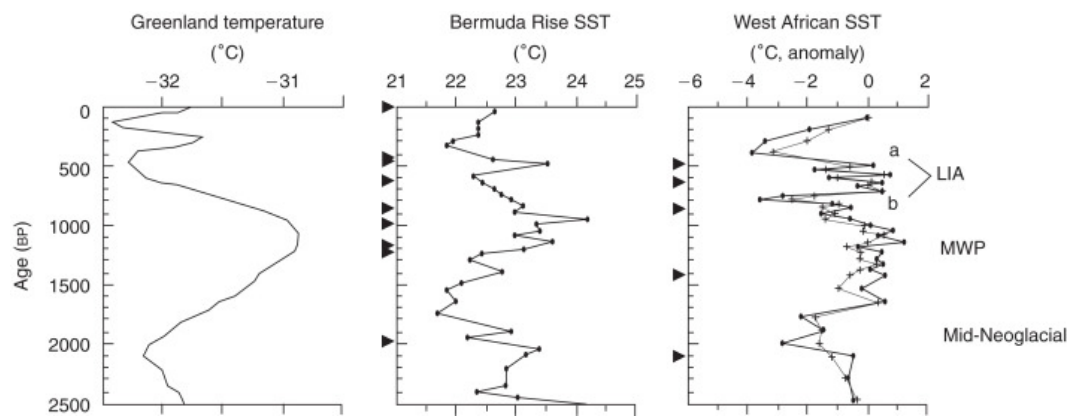


Figure 3. Comparison of Greenland temperatures, the Bermuda Rise sea surface temperatures (SST) (Keigwin, 1996), and west African and a sea surface temperature (deMenocal *et al.*, 2000) for the last 2500 years. LIA Little Ice Age; MWP Medieval Warm Period. Solid triangles indicate radiocarbon dates.

[> Read full chapter](#)

Geologic History and Energy

S.A. Elias, in [Encyclopedia of the Anthropocene](#), 2018

Atmospheric Impacts of Increased CO₂

The long-term effects of increased CO₂ in the world's oceans mean that even if humans stopped burning fossil fuels today, the [depletion](#) of CO₂ from the atmosphere that might otherwise be expected to take place would be delayed for many decades or centuries, as the oceans release excess back CO₂ into the atmosphere, maintaining the balance between oceanic and [atmospheric](#) CO₂ levels.

As has been documented during the last few decades, the increase in GHGs, especially atmospheric CO₂ and [methane](#), has caused significant warming of the atmosphere. As of 2016, the average global warming is 1.4°C above the long-term average for the 19th century (NASA, 2016). Most of this warming has occurred since the 1970s, with the 20 warmest years having occurred since 1981 and with all 10 of the warmest years occurring in the past 12 years (**Fig. 10**).

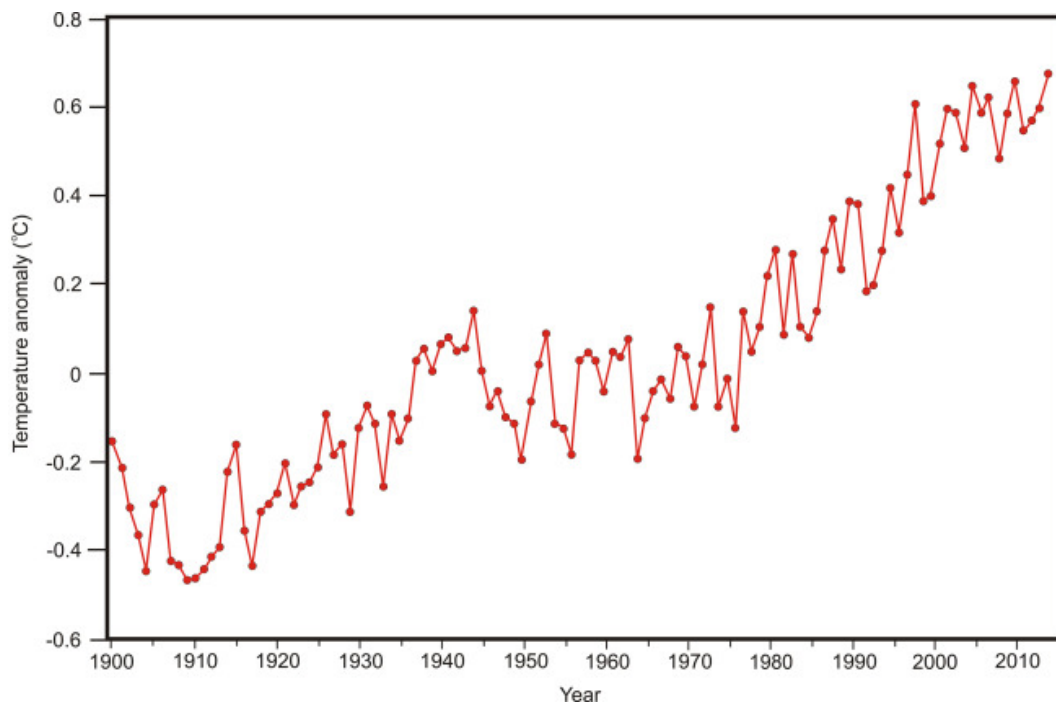


Fig. 10. Global temperature anomalies from 1900 to 2014.

Data from NASA-GISS (2016).

All of this heat originally comes from the Sun, but it should be pointed out that solar radiation is not constant. Increases in solar radiation can bring about temperature increases in [Earth's atmosphere](#). For instance, during the [Medieval Warm Period](#) (c.AD 1100–1200), increased levels of solar radiation are linked with temperature increases in the [Northern Hemisphere](#) on the order of 0.6°C. Conversely, lower than average levels of solar radiation (the so-called Maunder Minimum) that occurred from the mid-1600s to early 1700s are linked with temperature decreases in the Northern Hemisphere on the order of 0.6°C below the long-term average (Shindell et al., 2001). The first decade of this millennium witnessed a solar output decline resulting in an unusually deep solar minimum in 2007–09. Based on previous minima in solar radiation, [climate models](#) would predict a drop in surface temperatures on Earth, but in fact global temperatures continued to increase throughout that decade. This is just another indication that the high levels of GHGs in the modern atmosphere are now the most important driver of global climate change on this planet.

Another strong piece of evidence supporting the contention of climate scientists that global warming is being driven by GHG concentrations concerns the [orbital forcing](#) of climate change. Based on calculations first put forward by Milankovitch (1941), the current [interglacial](#) warm period that began about 12,500 years ago should be coming to an end. The long-term changes in [Earth's orbit](#) around the

Sun gave the planet a maximum of incoming solar radiation (insolation) during the early part of the interglacial, about 10,000 years ago (**Fig. 11**). In all previous Pleistocene interglacial periods, the levels of carbon-dioxide have dropped as the levels of [insolation](#) have declined, during the latter part of the interglaciation. As Ruddiman (2007) has pointed out, this makes the current interglacial (the Holocene) unique, and the difference must be the extra carbon-dioxide being pumped into the atmosphere by the burning of fossil fuels, in addition to the methane produced by livestock, decomposing vegetation in rice paddies, and methane being released from [thawing](#) sediments in the Arctic.

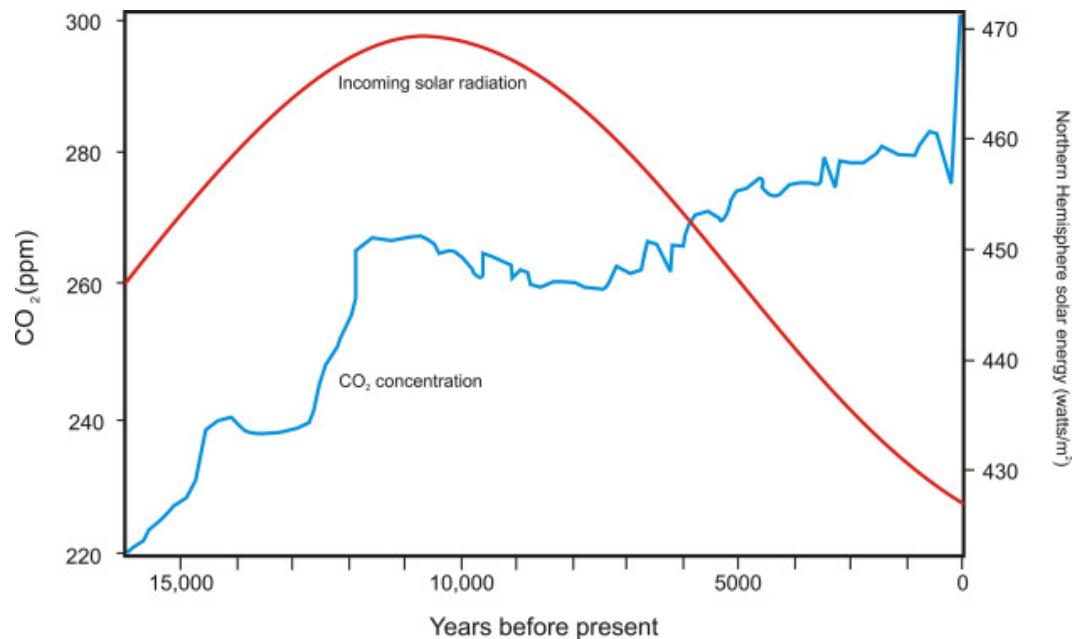


Fig. 11. Comparison of Holocene insolation (*red line*) with level of atmospheric CO₂ as recorded from the Antarctic Dome C ice core (*blue line*). Dome C ice core data from Blunier and Jenk, 2013.

[> Read full chapter](#)

Ground Temperature Histories: Evidence of Changing Climate

Louise Bodri, Vladimir Cermak, in [Borehole Climatology](#), 2007

Finland

Examples of the estimates of SAT [anomalies](#) for some [regions](#) of Europe extended back to approximately 1650 are presented in Figure 8 (Chapter 1). Smoothed values

were calculated from the data by Jones and Moberg (2003). Comparison reveals clear differences between illustrated regions. As shown, the range of variations of [temperature anomalies](#) is larger and the overall temperature trend is more pronounced in Fennoscandia rather than in Central Europe. On the other hand, the most dominant feature of the SAT at least in Finland is a strong interdecadal [variability](#) (Heino, 1994). While the [nineteenth century](#) appears as undoubtedly cold, the trends of the next century are less sure. The SAT record does not show any consistent warming or cooling.

All existing long-term paleoclimatic reconstructions in Fennoscandia are almost entirely based on the tree-ring proxies. Specific feature of the tree-ring method is that the low-frequency components may be damped because of the long response time of the tree to the weather variations and by the downward trends in growth associated with increasing tree age (see Section 1.2.3). Averaging the tree-width indices from many individual trees to gain continuous standardized record also effectively removes the long-term trends from the reconstructions (Sirén, 1961). Figure 84 presents the longest and most informative tree-ring series for pines at sites distributed over northern Finland for the period 1181–1960 A.D. (Sirén, 1961), i.e., from near the present northern forest limit. The record is highly variable even at the large scales of aggregation. The use of longer averaging periods reveals better long-term trends. The difference of this record from 2000 years' long temperature anomalies time series reconstructed for the [Northern Hemisphere](#) (Figure 3, Chapter 1) is obvious. Despite the short 20-year cooling events around 1450 and 1600 A.D., the data do not reveal any pronounced cold period that could be interpreted as the Little [Ice Age](#). Another 1400-year high-quality tree-ring record from Northern Sweden (Briffa et al., 1990) also indicates a relatively short Little Ice Age. Similarly, little evidence was obtained by Briffa et al. (1990) for the existence of the [Medieval Warm Period](#). It is not clear, however, whether these findings can be attributed to the real climatic conditions or to the above-mentioned loss of long-term trends from the tree-ring record.

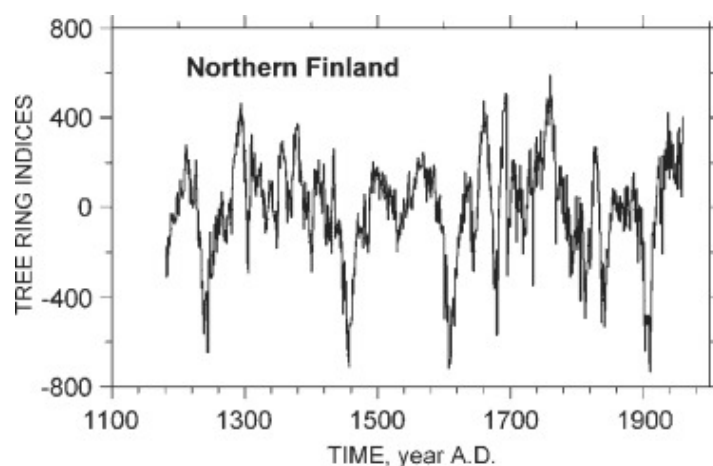


Fig. 84. Tree-ring width indices (in units of $1000 \times \log(M_g)$, where M_g is geometric mean of the tree-ring widths in millimeters) in northern Finland.

(From data by Sirén (1961).)

Copyright © 1961

Considerable progress was achieved in the 1990s in [borehole](#) paleoclimatic reconstructions for this area, when the data measured for the geothermal [heat flow](#) investigation were applied for climate studies. Three research fields were of special interest: (1) modeling of the [permafrost](#) in [bedrock](#) in northern Fennoscandia and its dependence on climatic variations (see Section 2.8), (2) evaluation of the long-term GST changes in deep [boreholes](#) (Section 3.5), and (3) the GST conditions in the last two millennia or so. Modeling of permafrost variations in northern Fennoscandia suggested rapid variations in permafrost thickness during the [Holocene](#) depending on the present ground temperature and past climatic variations (Kukkonen and Safanda, 2001). Obtained results have been described in detail in Section 2.8.

Observed vertical variation in the heat flow density in the Fennoscandian Shield and in the neighboring parts of the East European Platform was attributed to the major climate change at the Pleistocene–Holocene boundary, and the GST inversion results suggested an average warming of 8.0 ± 4.5 K from the [Last Glacial Maximum](#) time (Kukkonen and Joeleht, 2003, and the references therein). A significant vertical variation in heat flow density measured in a 12 km deep hole in the central part of the Kola peninsula was explained as arising due to the very low surface temperatures during the latest [glaciation](#) at times more than 10 000 years B.P. (Kukkonen and Clauser, 1994). Attempts to interpret temperature anomalies observed in Finnish deep holes will be described in more detail in Section 3.5.

Climate changes of the last 2000 years were inferred from three borehole temperature logs. Boreholes were situated within the narrow ($25\text{--}27^\circ\text{E}$) [longitude](#) strip in the northern (67.7°N), central (64.6°N), and southern (60.6°N) parts of the Finnish part of the Baltic shield. They were logged in the years 1988–1994 at least one year after the drilling had ceased. The measurements were performed with frequent readings (measured points were separated by a 2.5 m depth interval), and each record contains from 220 to almost 400 individual reading points. Measured temperature–depth profiles and reduced temperatures are presented in Figure 85. The bulk of the observed temperatures represent a [quasi-steady-state](#) geothermal field. As previously, to visualize temperature [perturbations](#) in measured profiles that might have been caused by climate change we used reduced temperature representation. As shown in Figure 85, departures from the steady-state conditions are significant only in the upper part of each hole up to the depth of 100–150 m. Below this depth reduced temperatures slightly oscillate around zero line. All reduced [temperature profiles](#) are

curved and systematically positive above 250 m depth with [amplitude](#) of 0.5–1 K indicating recent climatic warming.

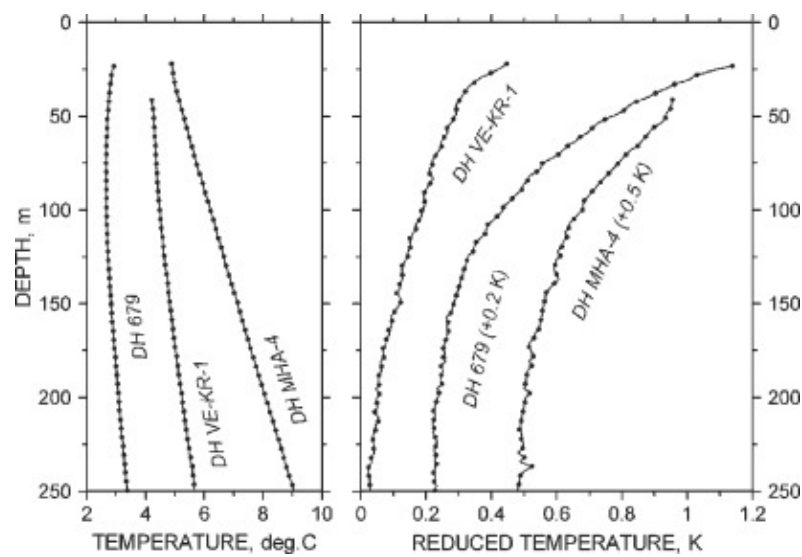


Fig. 85. Left: Temperature logs for three Finnish boreholes. Boreholes were logged to 570 m (DH VE-KR-1) and/or 920–950 m depth (DH 679 and DH MHA-4). Only upper 250 m depth interval is shown to emphasize “U-shape” of the profiles. Right: Reduced temperature profiles for Finnish boreholes.

All three temperature logs were inverted individually by SVD technique and for all of them the climatic episodes over the last 2000 years were identified. The method readily allows incorporation of additional information on both the measured data and the climate change. As was shown in Section 2.4.3 (Chapter 2), this procedure increases the number of parameters (individual intervals of constant temperature) that may be estimated. In addition, the information on decorrelation of the measured data and on the persistence of the climate changes has also been described (for details see Section 2.3.4). For all three investigated boreholes, a short-range dependence between data is characterized by a correlation that decreases exponentially fast. An example of the exponential decay of the [autocorrelation](#) function of the reduced temperatures is shown in Figure 86. The decorrelation distance, D , corresponds to the depth lag at which the autocorrelation decreases to $(1/e)$, and for all Finnish boreholes this was about 50 m. In other words, the individual measurements separated by this distance can be considered as statistically independent. Investigated boreholes represent relatively rare field example of boreholes with fast decorrelation (for comparison see Figure 35, Chapter 2; for Canadian borehole Hearst decorrelation distance equals 174 m; for the above-described Czech borehole HO-1 $D = 246$ m) and high number of measured points. Very effective technique of data thinning (“scarcing”) can be used for inversion of such T – z profiles. In this case the original dataset of measured temperatures can be divided into subsets, and different parameters of the time discretization of the GST history can be estimated from different sections of temperature log. This procedure significantly enhances

the number and reliability of estimated parameters but requires that the datasets used be statistically independent (Twomey, 1977).

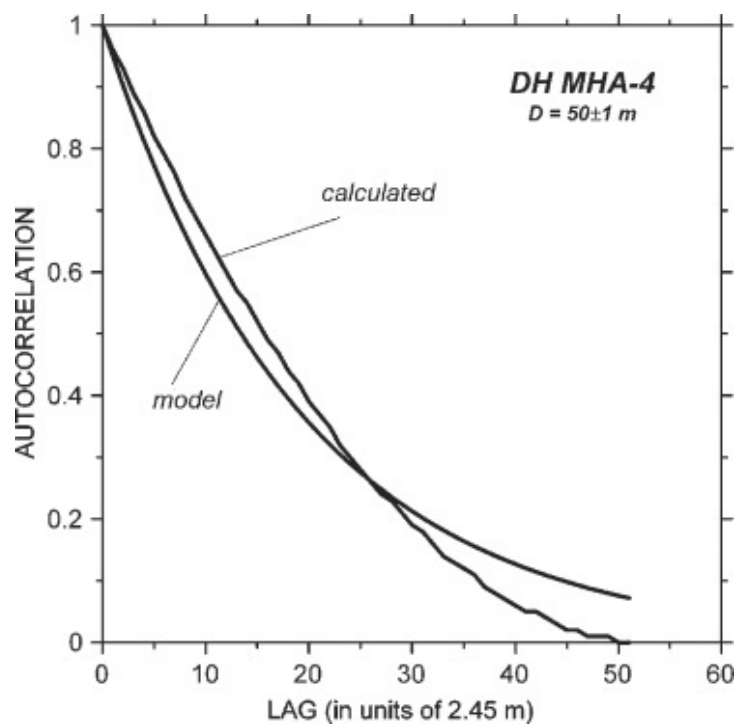


Fig. 86. Autocorrelation of measured temperatures at borehole DH MHA-4 in the interval of 34–162 m.

The reconstructed GST histories (Figure 87) appear to be coherent for DH679 and DH VE-KR-1 boreholes situated at more northern latitudes; however, some [incoherence](#) arises in the last 300-year part of the GST history obtained for DH MHA-4 hole, which cannot be regarded simply as an artifact of the solution. The GST history reconstructed for another Finnish borehole, Outokumpu (62.72°N, 29.02°E) done by Kukkonen and Safanda (1996), yielded results coherent with the DH MHA-4 GST history presented in Figure 87. These authors revealed cold episode 1000–1200 A.D., then warming culminated near 1750 A.D., subsequent cooling with its minimum at the year 1900, and warming since then. Certain explanation of the incoherence of the GST histories shown in Figure 87 can be looked for in the microclimatic local variations. Processing of further borehole temperature–depth profiles from the area will increase our knowledge on the [regional variations](#) of the Finnish climate.

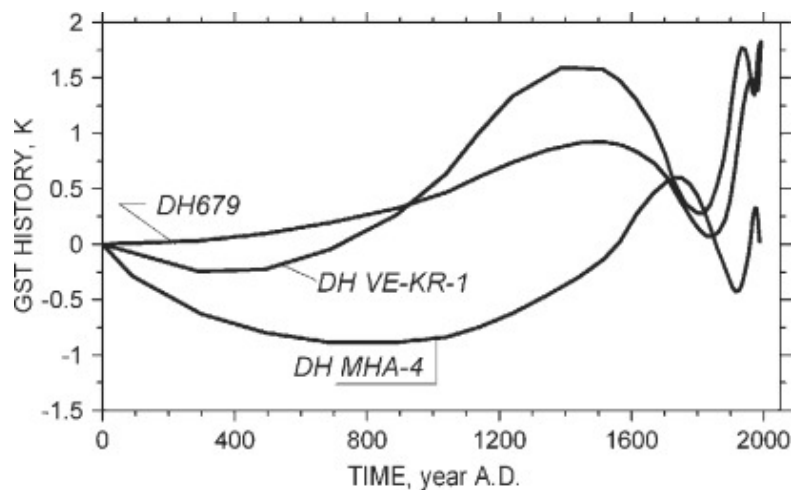


Fig. 87. Finland: Reconstructed GST histories.

As about two rest boreholes, the early section of the reconstructed GST histories generally covers a cold interval between approximately 400 and 1000 A.D., followed by a long gradual warming up to 1500–1700 A.D. and a cold period around 1800 A.D. While in Europe cold periods before 1000 A.D. and ca. 1800 A.D. are documented by a variety of proxy records, the fifteenth to [sixteenth century](#) warming in Finland appears to be different from the general European trend (see, e.g., Section 1.1, Chapter 1). Period from fifteenth to [seventeenth centuries](#) in Europe corresponded to the well-known cold conditions of the Little Ice Age. It should be mentioned that tree-ring record in Figure 84 also shows the years 1500–1750 as a generally warm time. Provisional return of cold near 1600 A.D. was probably too short to be resolved in the GST reconstructions that integrated all this period as a single warming event. It is not quite clear whether the prolonged time interval with culminating temperatures around 1500–1700 A.D. in Figure 87 can be simply interpreted as the Medieval Warm Period and the Little Ice Age shifted by 100–200 years. Anyhow, some distinction of the Finnish climate compared with the general climate course in Europe and/or the Northern Hemisphere can be observed not only for the last two centuries, but also probably for the longer times. Since there is no long enough series of the instrumental observations of temperature in Finland and/or the proxy records are also geographically and temporally discontinuous, the GST histories extracted from geothermal data may serve as a useful independent dataset to complete significantly the climate history of the [region](#). The amount of temperature logs measured in this area and their high quality provide the possibility to detect even more remote climate events and also their [spatial variations](#).

[> Read full chapter](#)